2012

DESIGN AND FLIGHT TESTING OF A WARPING WING FOR AUTONOMOUS FLIGHT CONTROL

Edward Brady Doepke
University of Kentucky, e.brady.doepke@gmail.com

DESIGN AND FLIGHT TESTING OF A WARPING WING FOR AUTONOMOUS FLIGHT CONTROL

_____

THESIS

_____

A thesis submitted in partial fulfillment of the
requirements for the degree of Master of Science in
Mechanical Engineering in the College of Engineering
at the University of Kentucky

By

Edward Brady Doepke

Lexington, Kentucky

Director: Dr. Suzanne Smith, Professor of Mechanical Engineering

Lexington, Kentucky

2012

ABSTRACT OF THESIS

DESIGN AND FLIGHT TESTING OF A WARPING WING FOR AUTONOMOUS FLIGHT CONTROL

Inflatable-wing Unmanned Aerial Vehicles (UAVs) have the ability to be packed in a fraction of their deployed volume. This makes them ideal for many deployable UAV designs, but inflatable wings can be flexible and don't have conventional control surfaces. This thesis will investigate the use of wing warping as a means of autonomous control for inflatable wings. Due to complexities associated with manufacturing inflatable structures a new method of rapid prototyping deformable wings is used in place of inflatables to decrease cost and design-cycle time. A UAV testbed was developed and integrated with the warping wings and flown in a series of flight tests. The warping wing flew both under manual control and autopilot stabilization.

KEYWORDS: Unmanned Aerial Vehicle (UAV), Wing Warping, Wing Morphing, Flight Testing

Brady Doepke
July 26, 2012

DESIGN AND FLIGHT TESTING OF A WARPING WING FOR AUTONOMOUS FLIGHT CONTROL

By

Edward Brady Doepke

<u>Dr. Suzanne Weaver Smith</u>
Director of Thesis

<u>Dr. James McDonough</u>
Director of Graduate Studies

<u>July 26, 2012</u>

ACKNOWLEDGMENTS

TABLE OF CONTENTS

LIST OF FIGURES

LIST OF TABLES

1   MOTIVATION

The Unmanned Aerial Vehicle (UAV) industry has grown over the past two decades at unprecedented rates. UAVs have found their way into defense, civil, commercial and personal uses. In the defense sector the Department of Defense (DoD) operates UAVs ranging from large reconnaissance UAVs at 60 thousand feet and small bird size UAVs deployed from a soldier's backpack [1]. Civilian organizations like the National Aeronautics and Space Administration (NASA) and the US Forestry Service operate UAVs to monitor atmospheric conditions and forest fires [2, 3]. Commercial groups have been trying to work their way into aerial photography and utility inspection, but growth remains slow due to ever changing laws in the US and abroad.   In recent years, the area of personal UAVs has grown with many open source projects leading the way by developing autopilot systems for hobbyists and UAV enthusiasts [4, 5].

UAVs open up several areas of the skies that previously were unattainable with manned aircraft. These areas are mainly high altitude, long endurance (HALE) aircraft in the upper atmosphere with potential for indefinite endurance, low altitude UAVs that can be easily packed and deployed, and UAVs for flight indoors or in confined areas. Each of these unique flight regimes can benefit from deployable wings. Rocket deployed HALE UAVs have been investigated as a means of rapid deployment option for ISR (Intelligence Surveillance Reconnaissance) missions. Small deployable UAVs like the Dragon Eye, Raven, and BATCAM are growing in use by the DoD [6].

Inflatable wings are one solution to deployable wing structures for UAVs. Inflatables offer a deployable option which is robust, highly packable, and shapeable for control. This last benefit offers a unique opportunity to use wing warping in place of conventional ailerons. Wing warping could offer benefits of reduced drag, reduced actuator power, and increased maneuverability [7, 8, 9].

For wing warping to be effective, the design must be efficient in the amount of power needed for actuation, reduce the drag of the wing and be able to change the wing's shape accurately enough for control. Several variables in the design must be investigated: warping method/how will the wing shape change, what kind of mechanism is going to be used for actuation, what does this mean for autopilot integration, and finally, how is this going to be developed for testing and use with inflatable wings?

The goal of this thesis is to design a warping wing for the purpose of testing warping methods to be used with inflatable wings for autonomous flight control. While the focus of this thesis is developing wing warping for roll control in place of conventional ailerons, much of what was learned and methods that were developed can easily be modified to work in place of elevators and rudders for pitch and yaw control.

In this thesis, Chapter 2 will present background literature on the history and purpose of wing warping, methods for warping, mechanisms for warping wings, a background on inflatable wings, and how wing warping effects will be measured, including aileron effectiveness and adverse yaw. Chapter 3 covers the design of a testbed aircraft for flight testing of the warping wing. In Chapter 4 details of how the warping wing is designed and built are presented. Chapter 5 covers ground testing that was done with the warping sections and the resulting changes made to the design. Finally, Chapter 6 covers flight testing done with warping wing sections. Chapter 7 provides a summary of the work and suggests future directions for the project.

2   LITERATURE REVIEW

2.1   Wing Warping

Wing warping is changing the shape of a wing for control purposes. Wing warping differs from conventional ailerons in that the shape change is continuous throughout a portion of the wing and not limited to a discrete area. It is also important to differentiate between warping and morphing. Wing morphing typically involves large changes in the wings planform to drastically change the optimal flight regime of the aircraft, compared to warping which is for control purposes.
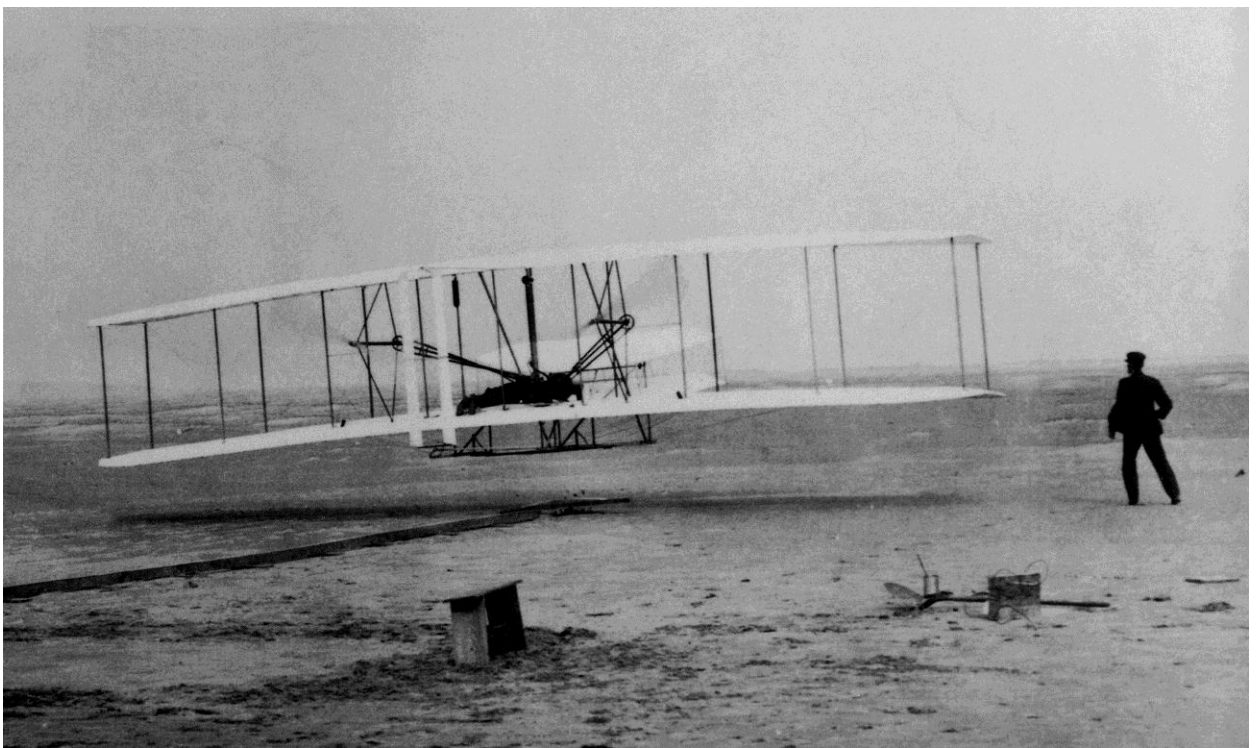
Figure 2-1: Picture of 1903 Wright Flyers maiden flight December 17th 1903 Kitty Hawk NC [10]

Wing warping for flight control has been around longer than manned flight itself (Figure 2-1). Wing warping made Orville and Wilbur Wright's 1903 Wright Flyer's first flight possible on December 17th 1903 (Figure 2-2) [11]. Their warping mechanism was perfected through tests of the 1902 glider and was the main claim in the brothers' first patent filed eight months before the first flight of the Wright Flyer(Figure 2-3) [12, 13].

Figure 2-2: 1903 Wright Flyer showing warping wings [10]
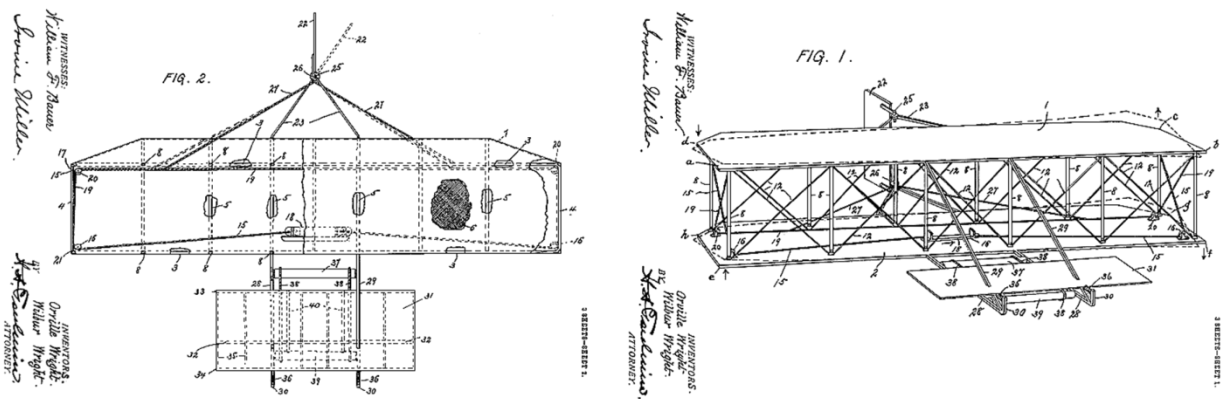
Figure 2-3: Drawing from the Wright's first patent for wing warping [12]

Despite that wing warping was the final piece of the puzzle for controlled flight, a decade after the Wrights' first flight, wing warping was gone and the hinged aileron had taken its place. As aircraft increased in speed, the low torsional stiffness needed for twisting the wings caused complications with aeroelasticity leading to flutter [14]. Interest has progressively turned back to warping with potential benefits in actuation energy efficiency, reduced drag, and increased maneuverability.

A paper by Johnston, et. all, showed that by using vortex lattice method and strain energy to model aerodynamic and control actuation forces, an optimal solution using wing warping existed [8]. Work done by Guiler using warping wing tips for flight control showed a 15% decrease in L/D compared to conventional control surfaces in wind tunnel tests. A radio controlled (RC) flight demonstrator was also successfully flown [15].

4

A joint NASA, Air Force Research Laboratory, and Boeing Phantom works project used a modified F/A-18 with flexible wings as part of the Active Aeroelastic Wing (AAW) project [16]. By developing the control system for the flexible wing, future aircraft can be designed with high aspect ratio, low stiffness, and low weight wings that can still be controlled. The AAW aircraft was able to achieve roll rates within 15 to 20% of a standard F/A-18 [16]. On a different scale researches are using wing warping for a highly maneuverable micro-aerial vehicle (MAV) achieving 200°/s roll rates [9].
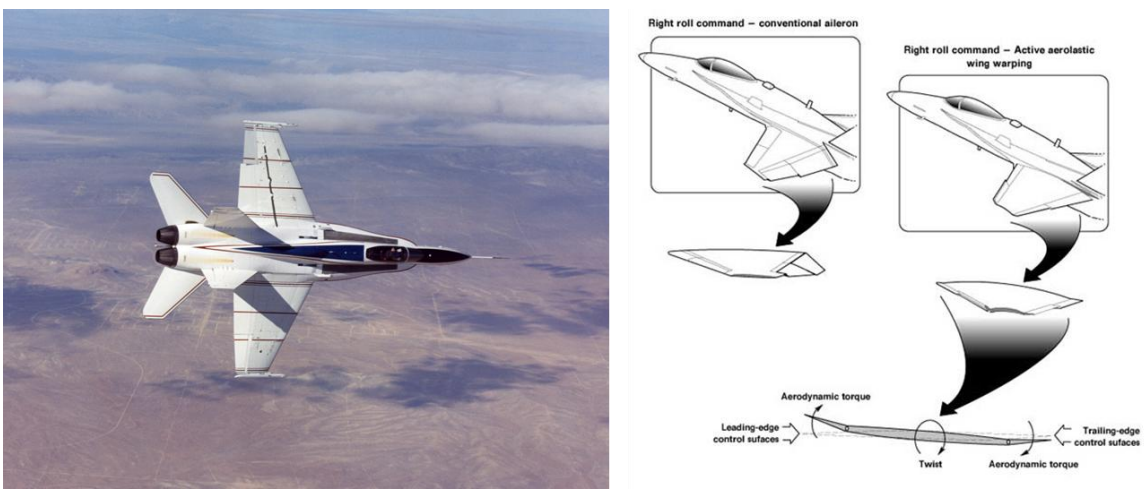
Figure 2-4: Left) AAW Aircraft Right) Sketch comparing AAW to conventional ailerons [16]

2.2   Warping Methods

There are several different ways to change the amount of lift produced by a wing for roll control. This thesis focuses on wing warping, sometimes called wing shaping, which is small changes to the cross section shape or orientation to the flow of the wing at one point or across the entire span. Most of these methods can be broken down into three groups [17].
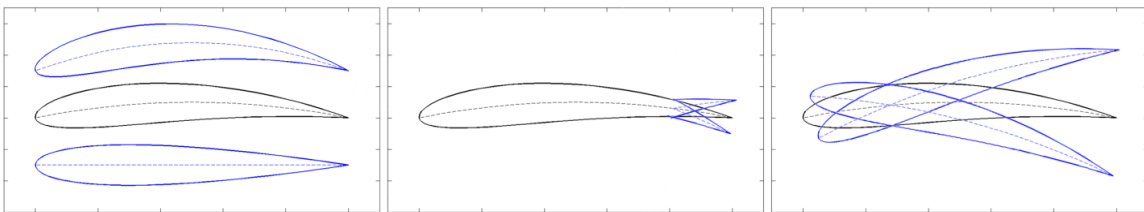
Figure 2-5: Three wing warping methods A) Camber control B) Single point bending C) Twist

5

Camber control (Figure 2-5 A) changes the camber of the wing to increase or decrease the amount of lift produced. The actuation affects the entire cross section of the wing moving both trailing edge (TE) and leading edge (LE).

Single point bending control (Figure 2-5 B) is similar to camber control in that the cross section of the wing is deformed, ultimately changing the camber. Single point bending only changes the camber of the wing at one point. The camber curves about a single point while the rest of the cross section remains fixed.

Twist control (Figure 2-5 C) takes a portion of the wing and twists it about a point, ideally keeping the same cross section. This changes the angle of attack (AoA) of the wing continuously along the span between a fixed point with the original AoA and the actuated portion with a positive or negative AoA. This changes the shape of the wing along the span between the point being twisted and a fixed portion of the wing.

2.3   Mechanisms for Wing Warping

For each warping approach there must be mechanisms to control the shape of the wing. These mechanisms can be categorized as external, internal, and integral. They can also be considered fixed or floating mount. Some methods discussed below have been implemented on non-inflatable wings, but the methods used could still be applied with modification

2.3.1   External Actuation

External actuation is a mechanism placed predominantly on the outside of the wings surface and applies forces to the outer surface. External actuation has been used for camber control of inflatable wings was accomplished by mounting servos to large pads on the inflatable wing's surface and using linkages to bend the wing (Figure 2-6 & Figure 2-7). Both wings have been flight tested successfully under RC [18, 19]. These are floating mechanisms since they do not require mounting to a rigid structure.

Figure 2-6: UK inflatable wing with external actuators
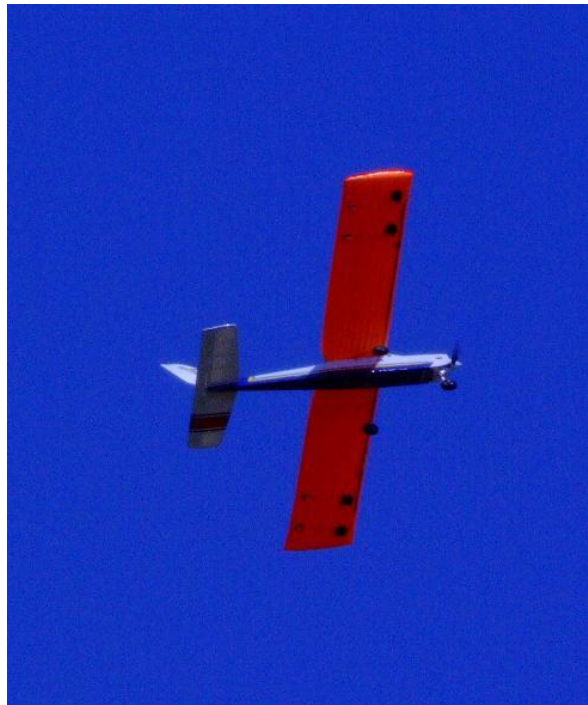
Figure 2-7: Oklahoma State University (OSU) using external actuation to control inflatable wings [19]

A wing warping system developed for micro-aerial vehicles (MAV) uses Kevlar strings running from points on the wings' surfaces to servos inside the fuselage to warp the wing (Figure 2-8) [20]. This method is considered a fixed mechanism since it does require the mechanism be mounted to the structure of the fuselage. This MAV was successfully flown under RC control. Closed loop controllers were designed and used in simulation but were not able to be integrated due to the small size of the aircraft. New hardware plans were made to implement closed loop control, but not complete [21].

Figure 2-8: University of Florida (UF) MAV using strings to curl the wing [9]

2.3.2   Internal Actuation

Internal actuation places the mechanism inside of the deformable part of the wing and the forces are applied from within. In the case of inflatables this would be inside the pressurized surface. The wing tip in Figure 2-9 is part of a morphing aircraft wind tunnel model. The tip is made from polyurethane foam and twisted by an internal pneumatic actuator capable of 113 in-lbs of torque [22, 23]. This would be considered a fixed mount mechanism meaning that the actuator located in the wing needs to be mounted to the rigid structure in the wing. This model was wind tunnel tested and a flight model was not developed.

Figure 2-9: VT compliant twisting wing [22]

Another twisting design used a rigid spar and rib structure covered in an elastomeric skin. Results showed that the twisting design increased the AoA envelope of the wing when compared to a conventional control surface (Figure 2-10) [24].
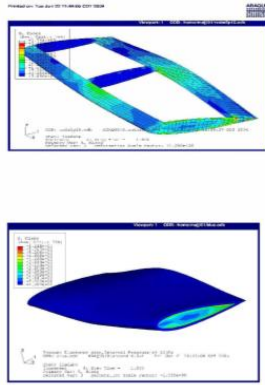
Figure 2-10: Texas A&M morphing wing [24]

2.3.3   Integral Actuation

Integral mechanisms are ones built directly into the wing's surface. They do not have structure internally or externally. This area has potential for integration of electro-active fabrics and piezoelectric actuators.

Nitonal wire on the wing's surface was used to contract and deform inflatable wing's (Figure 2-11). Nitinol is a smart material that, after being deformed, can be heated, in this case by electrical current and will return to its original shape. But due to severe actuation lag the system was never flight tested [18].

Figure 2-11: Left) Nitinol actuator for an inflatable wing-Right) Actuated and zero deflections [18]

ILC Dover also worked with actuating inflatable wings with several different methods. Figure 2-12 shows one method of using piezoelectric actuators to warp a fabric-skinned portion of the TE of an inflatable wing. This design was shown to provide adequate deflection and quick response for use in roll control [25].However this design was never flight tested.

| Bench Top Mockup with Covering | Segmented Piezo Actuators - Cover Removed | Piezo Actuated Trailing Edge Side View |

Figure 2-12: ILC Dover piezoelectric actuated trailing edge on a Vectran infltable wing [26]

Another study looked at using Macro Fiber Composite (MFC) actuators to shape the wing's surface (Figure 2-13). Several RC flight tests were performed with mixed results. The aircraft was able to achieve stable flight but the morphing controls had low control authority. Bilgen states that this was likely due to wing oscillations that were the result of the relatively low wing stiffness needed to allow the MFC actuator to work [27].
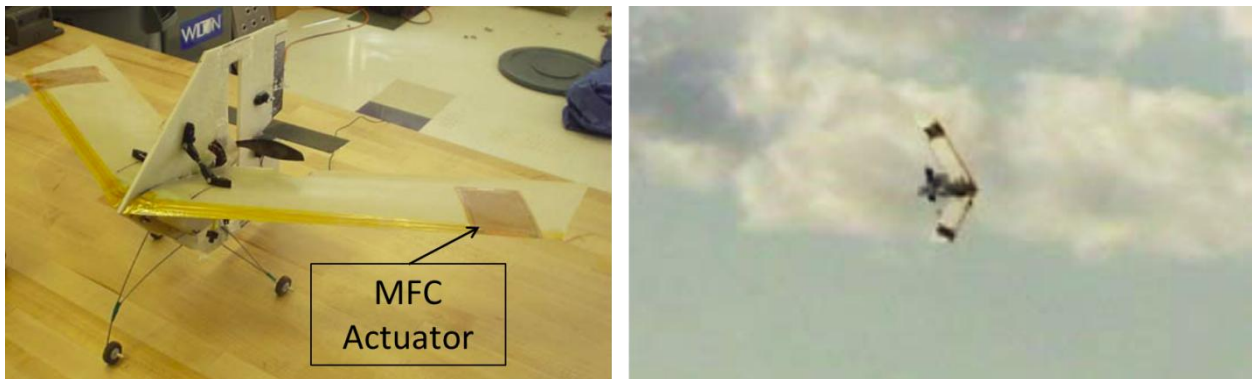
Figure 2-13: MFC Actuated UAV [27]

2.4   Inflatable Wings

Inflatable wings and even inflatable aircraft have a long history. The earliest examples include lighter than air (LTA) vehicles such as blimps. This review will focus on inflatable structures used for lift generation and not LTA vehicles. A patent in 1930 was filed for the use of

inflatables as the main spar for an aircraft [28]. The next step in inflatable wings came in the 1950's with the Goodyear Inflatoplane (Figure 2-14 Figure 2-15).
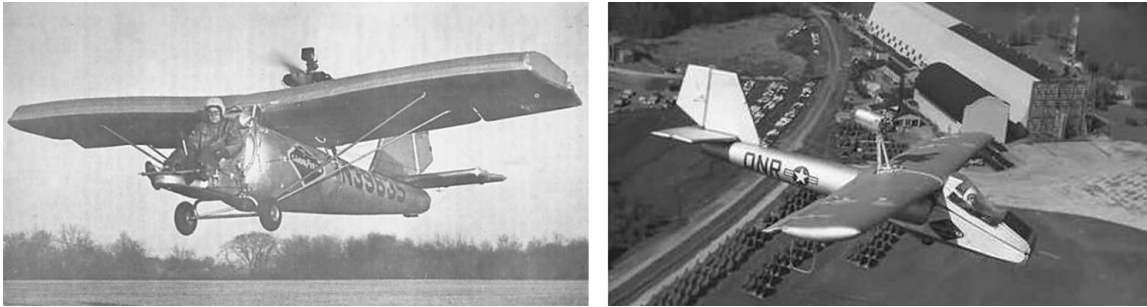
Figure 2-14: Goodyear Inflatoplane [18]
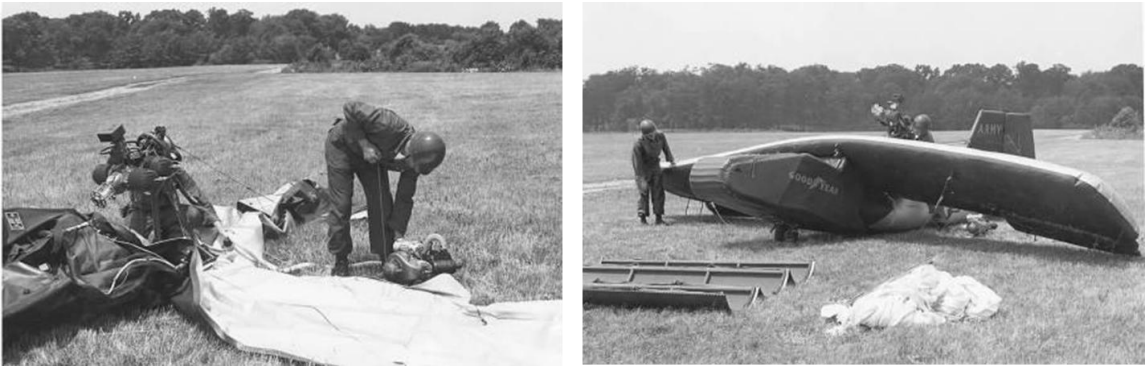
Figure 2-15: Inflatoplane being deployed by a single solder [18]

The Inflatoplane was developed as a rescue plane to be dropped from the air to a downed pilot in enemy territory in a packed configuration. A single person could deploy and fly the Inflatoplane to friendly territory. Multiple versions were created and flown successfully. But low torsional stiffness led to aeroelastic divergence and eventually wing buckling [29].

In the 1970s ILC Dover developed the first inflatable wing UAV (Figure 2-16) with a 5ft span and 7lb gross takeoff weight (GTOW) called the Apteron. The UAV was successfully flown under RC by using rigid elevons on the trailing edge [26]. ILC Dover later continued development of inflatable wings and is covered in Section 2.4.1.

Figure 2-16: Apteron inflatable wing UAV by ILC Dover [26]

Both the Apteron and Inflatoplane offered packable options for deployable aircraft. In a survey of deployable wing systems by Harris [30], inflatable wings were shown to have packing ratios of 10% or less. Harris showed that inflatable flexible wings offer significantly better packing potential when compared to hybrid (inflatable with rigid components) and rigid deployable wings (Figure 2-17).
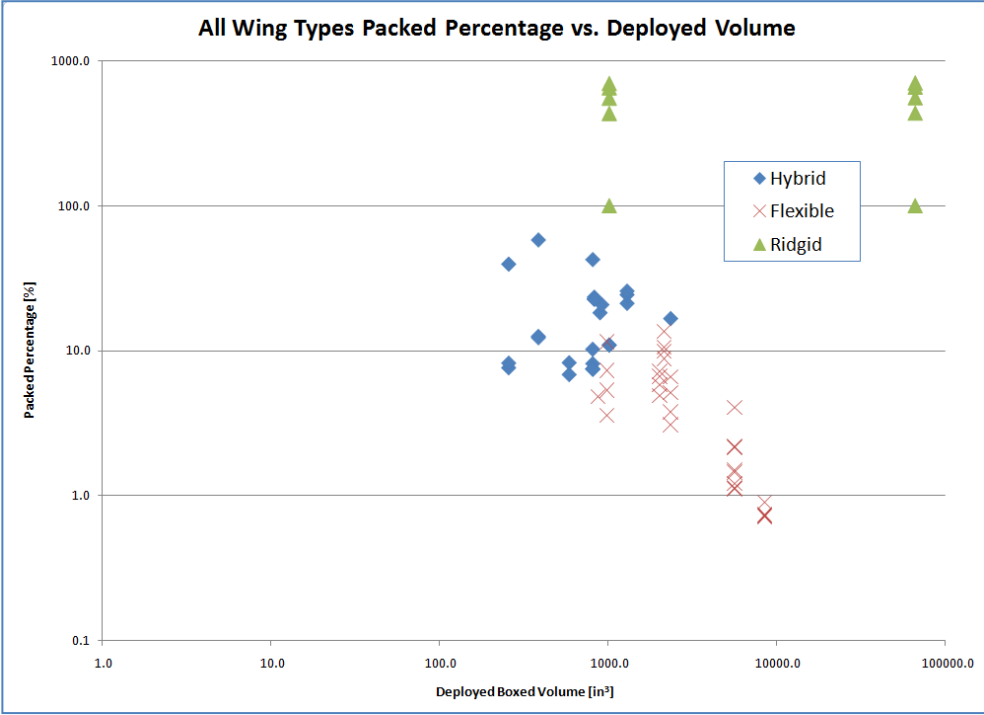
Figure 2-17: Comparison of packing ratios of deployable wing systems [30]

2.4.1   Inflatable Wing Research at The University of Kentucky

From prior research, several inflatable wings were available for testing (Figure 2-18) [18, 31, 14].   These wings served as the starting point for development of the wing warping mechanism in this study.

Figure 2-18: Inflatable wings available at UK [18]

None of the inflatables in Figure 2-18 were manufactured with the intent of being used for wing warping. In flight testing between 2002 and 2007, most vehicles used a split elevator also called a elevon for roll control, or rigid conventional ailerons were attached to the TE of the wing.

Later some wings were modified for wing warping [18, 19]. The wings shown in Figure 2-19 were modified by Simpson [18] to have floating external servos for camber control. Several RC flight tests were flown with the wings on a small airframe known as a Duraplane [18, 31].

Figure 2-19: UK Inflatable wings with external floating camber actuation

In 2009, The University of Kentucky-Dynamics Structures and Control lab began work with NextGen Aeronautics (NextGen) on a project developing a rocket deployable UAV for a High Altitude Long Endurance (HALE) mission [32]. The confines of the rockets along with the HALE requirements meant that a high aspect ratio wing with a high packing ratio needed to be designed.

13

NextGen decided to use a hybrid deployable wing with inflatable and rigid deployable sections. The design called the Stowed Unmanned Air Vehicle Engineering (SUAVE) used a telescoping main spar with rigid ribs spaced between 3 and 4 chord lengths (Figure 2-20) [33]. Unlike the inflatable wings in Figure 2-18 which used the inflation pressure and fabric to carry the structural load, the SUAVE design uses the spar to carry the load and the inflatable to maintain the wing's shape.
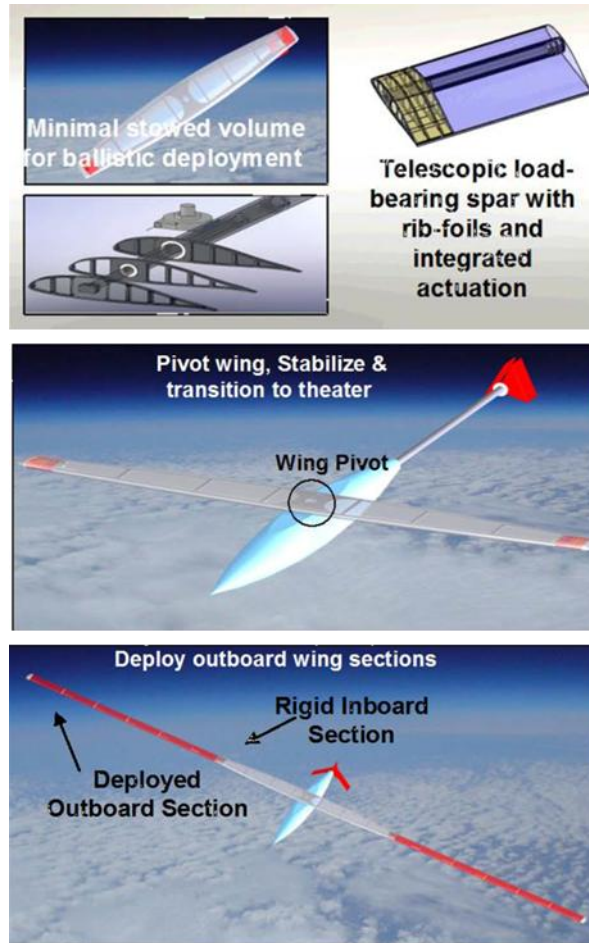
Figure 2-20: Concept for deployable HALE UAV with hybrid inflatable/rigid wing [32]

Two scaled models of the SUAVE design were tested for dynamic deployment in high altitude vacuum chambers (Figure 2-21). The largest was made had a stowed length of 2.5ft and deployed length of 10ft. It consisted of a rectangular telescoping pneumatically deployed main spar with five ribs and four inflatable sections [32]. The rigid structure inside the inflatable makes this design ideal for integration of wing warping mechanisms. The fixed ribs could easily

be replaced by actuated ribs with either camber control or single point bending. The spar could be actuated to rotate one the ribs for a twisting control.
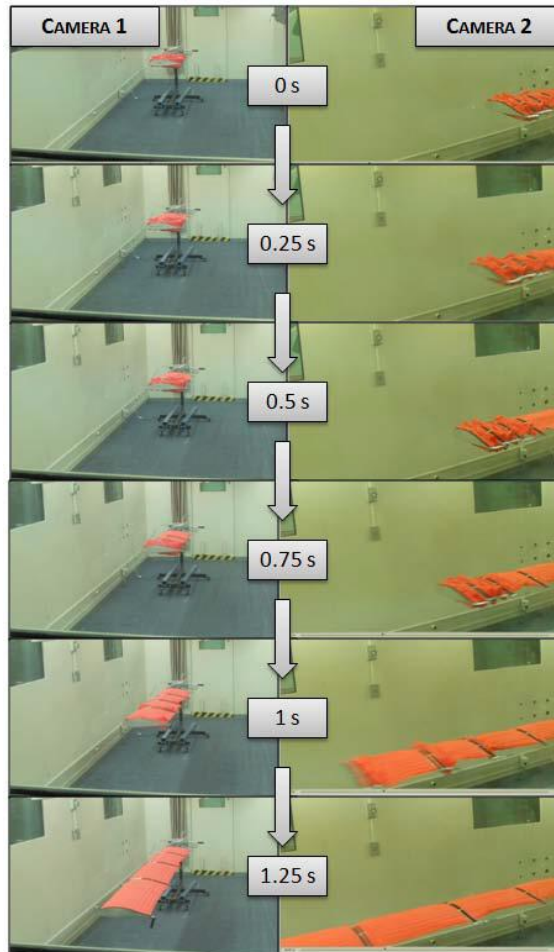
Figure 2-21: SUAVE Subscale deployment model being deployed in high altitude conditions [32]

2.5 Aileron Effectiveness

In order to quantify the performance of the ailerons or warping, the aileron effectiveness will be calculated. The aileron effectiveness is the primary parameter used in an autopilot to design controllers for the aircraft. This same parameter will be used to characterize the performance of the warping actuation. For this reason the term aileron effectiveness will be used to describe both aileron and warping effectiveness.

The aileron effectiveness is a comparison of how the aircraft responds in roll to a given input from the ailerons. The roll rate of the aircraft must be nondimensionalized in order to

make comparisons at different velocities and with different size aircraft. Dimensionless roll rate $\bar{p}$ is defined as [34].

$$\bar{p} \equiv \frac{pb_w}{2V_o} \tag{2-1}$$

The dimensionless roll rate is the result of normalizing the roll rate (p) in radians/s by the aircraft's wingspan b_w and the free stream velocity V_o. Aileron effectiveness is defined in the Piccolo™ autopilot manual as the difference in dimensionless roll rate divided by the difference in aileron deflection over a period of time with fixed aileron input [35].

Using the gyro, indicated air speed (IAS), and control surface positions recorded by the aircrafts telemetry units see Section 3.4, the aileron effectiveness can be calculated by performing a maneuver called a doublet. From steady level flight, the aileron is deflected one direction and then deflected the other direction and the response measured. During the maneuver, the other controls are kept fixed at their trim positions. Figure 2-22 shows example telemetry during a typical doublet maneuver and the points used in (2-2) for determining aileron effectiveness.

$$Aileron\ Effectivness \equiv \frac{\bar{p}_2 - \bar{p}_1}{\delta_2 - \delta_1} \tag{2-2}$$
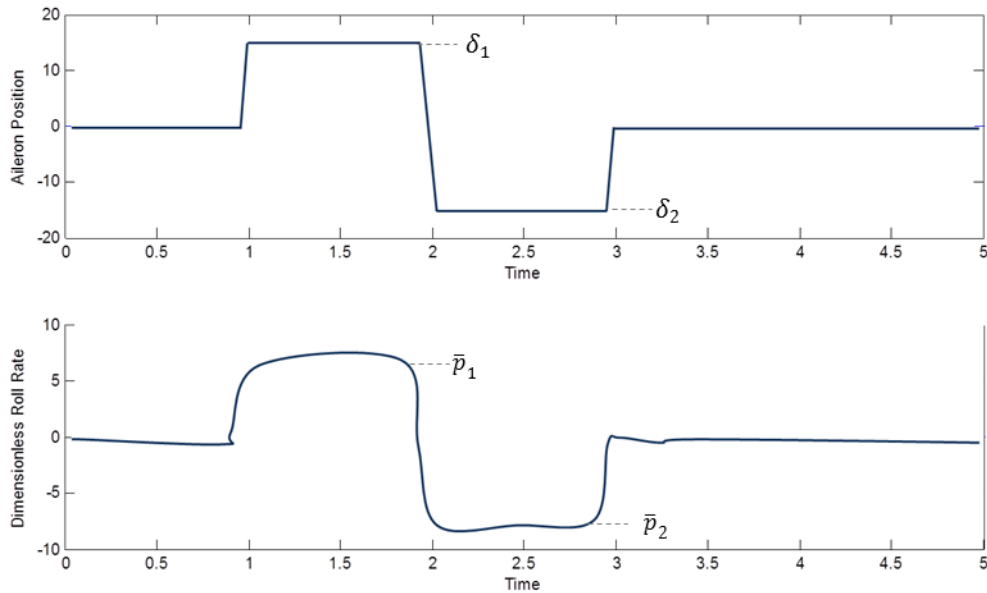
Figure 2-22: Telemetry showing values used in Equation (2-2)

16

2.6   Adverse Yaw

When an aircraft initiates a turn, for example to the right, the right aileron deflects upward and the left aileron deflects downward. This creates a moment in the roll direction towards the right. It is common for aircraft to then experience a yawing motion in the opposite direction, in this case to the left. This is called adverse yaw. Adverse yaw is the result of the difference of the induced drag between the left and right wings. In the case of the right hand turn, the right wing decreases its lift, which results in less drag. The left wing increases its lift to move upward and increases its drag. This difference in induced drag results in the opposite yawing moment. Similar effects are also true for left turns. In order for an aircraft to perform a coordinated turn, meaning flight with no sideslip and maintaining acceleration perpendicular to the z direction, the pilot uses the rudder to generate a yawing moment to align the nose with the flight path, overcoming adverse yaw.

In addition to aileron effectiveness, measuring the amount of adverse yaw caused by the ailerons or warping will help quantify the aircraft's roll performance and control. The yawing moment N for the entire aircraft can be non-dimensionlized using

$$C_n \equiv \frac{N}{\bar{q}Sb} \tag{2-3}$$

where C_n is the non-dimensional yawing moment, s is the planform area of the wing and b is the aircraft wingspan. The quanity $\bar{q}$ is the dynamics pressure defined as

$$\bar{q} \equiv \frac{1}{2}\rho V^2 \tag{2-4}$$

where ρ is the atmospheric density and V is the free stream velocity.

Depending on the configuration of the aircraft and the necessary accuracy of the model C_n can be a function of almost any parameter. However for aircraft of typical configuration, it is historically shown that C_n is dependent on side slip angle β, roll and yaw rates p, r, and aileron and rudder deflection δ_l, δ_n [36]. If these dependencies are considered linear about some stable condition of the aircraft, an equation for C_n can be made which is the sum of the partial derivatives of C_n with respect to each variable multiplied by the difference of each variable from the stable condition [36].

$$C_n = \frac{\partial C_n}{\partial \beta} \Delta\beta + \frac{\partial C_n}{\partial p} \Delta p + \frac{\partial C_n}{\partial r} \Delta r + \frac{\partial C_n}{\partial \delta_l} \Delta\delta_l + \frac{\partial C_n}{\partial \delta_n} \Delta\delta_n \qquad (2\text{-}5)$$

2.7 Literature Review Summary

From examining past work it is clear that inflatable wings offer a highly packable option for deployable wing systems, particularly for small to medium size UAVs. Inflatable wings have been used successfully and flown under RC control and even under autonomous control when using conventional elevons. While inflatables come with complications for conventional control surfaces, they have the opportunity to integrate wing warping for control.

Several methods of wing warping and mechanisms for warping have been evaluated. Different levels of testing ranging from computational simulations to flight testing have been done with wing warping for flight control. While warping wings have been RC flown as part of both inflatable and non-inflatable wing aircraft, at this time the author is not aware of any wing warping flights performed under autonomous control.

This thesis will cover the development of an autonomous platform, the manufacturing of a warping wing, and the integration and flight testing of a warping wing aircraft.

3 AIRFRAME TEST BED DEVELOPMENT

With the final goal of an autonomous flying aircraft with warping wings, it was important to find an airframe capable of testing the warping wings that can be easily be adapted to accommodate design changes. It was important that the aircraft have conventional wings to be used during the checkout of aircraft systems and as a control condition to compare conventional ailerons to wing warping. The test bed refers not only to the flying airframe but also all of its sub components, ground station, and support equipment necessary for flight operations.

The test bed was developed prior to the warping wing, meaning that the airframe design will drive the wing design but not vice versa. While this constraint does limit the design space of the warping wing it does help speed up the design process by eliminating variables. The test bed is meant to serve not only this thesis project but other projects in the UK UAV Lab, such as the including a project where it is used for flying cameras for 3D scene generation and networking payloads.

3.1 Test Bed Requirements

Several requirements drove the design and selection of the components for the airframe and avionics. The selected airframe had to be able to carry 4-6lbs of additional weight to accommodate avionics, extended tanks/batteries, and heavy prototype wings. The design had to be rugged and able to handle rough landings and modifications to the fuselage for camera mounting and payload placement. The ability to acquire and construct a new airframe helps with quick turnaround after repairs. Using commercial off the shelf (COTS) parts allows for easy maintenance and quick field repairs.

The design was a high wing design for passive stability. The wing mounting had to be easily adapted to accept different wings. The propulsion had to be quickly adapted and optimized based on the mission requirement and gross takeoff weight (GTOW) of the aircraft. The avionics needed to provide fully autonomous flight with two-way real-time telemetry. The system also needed to have a minimal lag RC-backup for the safety pilot. In order to record data for determining aileron effectiveness, the system needed to be able to record global positioning system (GPS), IAS, servo position, acceleration, and angular rates.

3.2 Airframe

The airframe selected for this project was the Hobbico NexStar™ (Figure 3-1). Previous work with the NexStar in the UK UAV Lab showed it to be a versatile platform well suited for carrying payloads. The airframe is commonly used as a trainer for RC pilots which means the flying characteristics are inherently stable and predictable. Previous flight testing had shown the airframe is also designed to survive rough landings and some crashes. The overbuilt design and sturdy construction of the fuselage allows for large access hatches to be cut and many modifications to be made without compromising the structure. The wings provided with the NexStar have been flown in flight tests at UK with a GTOW of 12lbs.

Figure 3-1: UK NexStar converted for autonomous operation

The NexStar was also used as the airframe for the Research and Engineering Center for Unmanned Vehicles' NexSTAR UAS (Figure 3-2). Some of the modifications made to the NexStar at UK are based on those presented in a manual made by the RECUV lab for NexStar conversion [37].

Figure 3-2: NexStar UAS at UC-Boulder RECUV Lab (www.recuv.colorado.edu) [38]

The use of a COTS platform had the benefit of lowering cost and manufacturing time. A NexStar airframe can be completed and ready for avionics integration in two days with a total cost of $800. This, along with the additional benefit of interchangeable parts, makes it ideal for a flight test bed. Repairs can often easily be made in the field.

Several modifications were made to the stock NexStar. Elevator and rudder servos were moved to the tail to open up the area directly below the center of gravity (CG) for avionics and payload (Figure 3-3). Additional power switches for servo and avionics power were installed along with ports to power the testbed from ground batteries during preflight checks (Figure 3-3). The control for the nose gear was also moved to open the payload area (Figure 3-4).
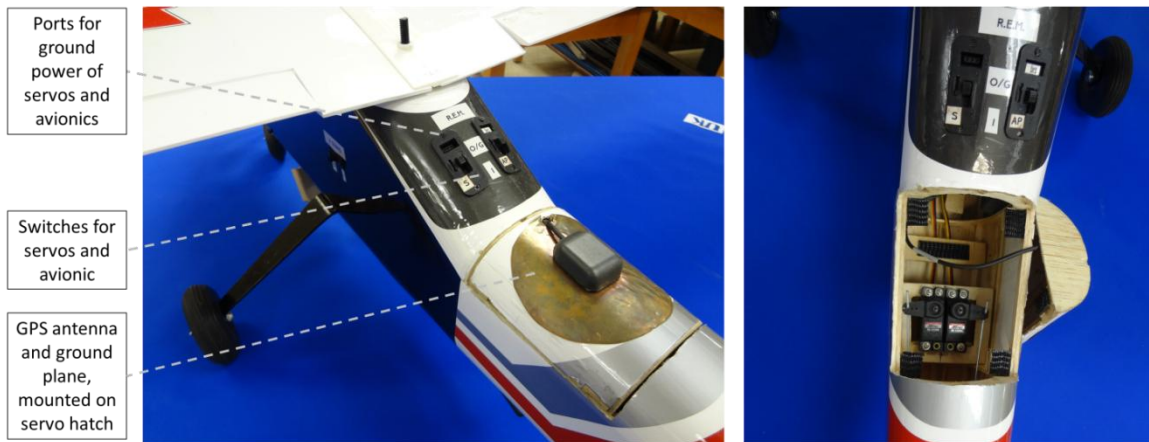
Figure 3-3: Left) Aft modifications and power control switches Right) Servos moved aft for increased payload volume
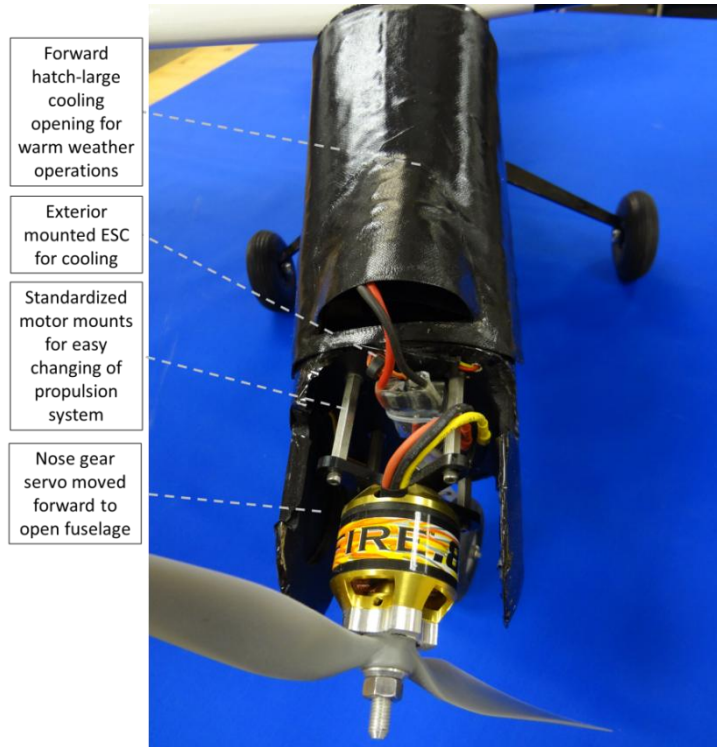
Figure 3-4: Forward modifications, electric motor, modified nose gear, and forward hatch

A front access hatch was added to place batteries and other components. The replacement hatch was designed with an air scoop to capture flow aft of the propeller for cooling of the batteries, avionics and payload. A hatch without an opening is used in winter weather. The term NS platform refers to the aerial platform and all of its avionics and systems. NexStar will refer to the airframe as is from Hobbico.

3.3 Propulsion Selection

The requirement for propulsion was to provide a reliable and easy-to-work-with system that can be adapted to fit missions' needs (endurance, speed, etc.). Originally the NexStar is equipped with a 0.46in^3 nitromethane glow fuel engine. This, along with other engines and electric motors, were considered for use in the testbed.

3.3.1 Gas Engines

Figure 3-5: Glow engine NexStar used for pilot training

Small gas RC hobby planes like the NexStar typically operate on 2-stroke glow engines burning a mixture of nitromethane and oil lubricant. NexStars were flown with the stock $0.46in^3$ and $0.55in^3$ glow engines to evaluate their potential for use in the testbed (Figure 3-5). Despite the low cost and long flight times, several issues were identified with the glow fuel systems.

The two stroke operation means that uncombusted oil is expelled out of the exhaust. This oil, despite being routed through the exhaust pipe out the bottom of the aircraft, still creates a slippery film on the outside of the aircraft potentially getting on cameras mounted on the aircraft. Small leaks in the fuel lines inside the aircraft and small gaps in hatches means that fuel/oil can also get inside the fuselage and potentially contaminate electronics.

The forward placement of the original fuel tank meant that an extended tank could not be used since the change in CG of the aircraft as fuel is burned would be too great. Mounting the tank at the CG proved impractical since this was originally intended to be the payload area so that the aircraft can fly different weight payloads and not require ballast.

Integration of the engines with the autopilot system also proved difficult due to vibrations and throttle control. Vibrations from the engine caused the autopilot gyros to become saturated. Various dampers were tried and vibrations were reduced just below the necessary threshold for operation but the vibration was still very strong, adding noise to accelerometer and gyro data. These vibrations could also cause blurry images with camera payloads.

The autopilot also had difficultly controlling the throttle of the engine. Since glow engines don't have an ignition system it can be difficult to maintain combustion with simple throttle settings. Usually, when under RC control, the pilot can listen to the engine and gauge where idle should be or when the engine is about to cut-out due to extended idling periods. This required constant adjustment of the throttle settings within the autopilot.

Gas engines also require routine maintenance and adjustments in the field. Often engines can have trouble starting, particularly in cold weather or after long periods without being run. Operation of gas engines also requires a depth of knowledge about the engines that is not required for electric motors.

While solutions exist to solve many of these issues, and despite the potential benefits in range and quick turnaround, the decision was made to look into electric systems. Other internal combustion engines (4 stroke, capacitive discharge ignition, etc.) were considered but not tested due to the added weight, cost and complexity.

3.3.2 Electric Motors

Use of electric motors in the hobby RC community has increased greatly over the past decade with advancements in battery technology [39]. A typical electrical system consists of a propeller, electric motor, ESC (electronic speed controller), and LiPo (Lithium Polymer) battery (Figure 3-6).
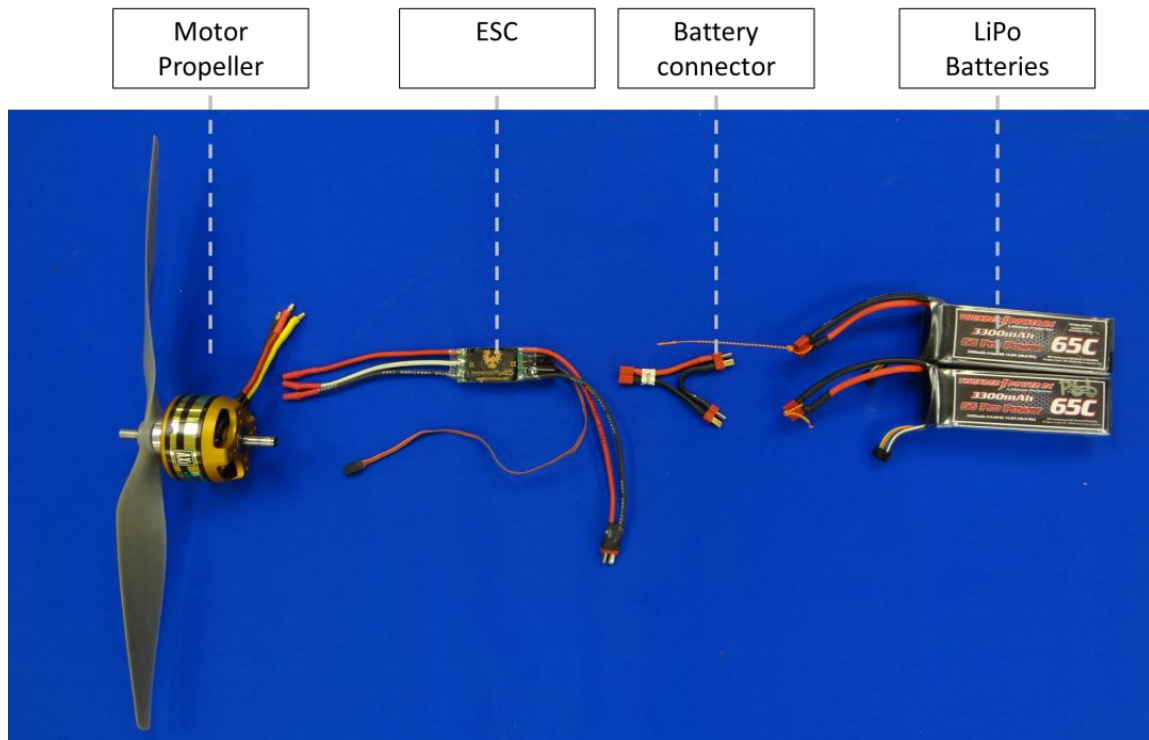
Figure 3-6: Components of typical electrical setup

Several electric configurations were evaluated in wind tunnel and flight tests. The electric motor units performed at the same level as the glow engines but without the complications of autopilot integration and many of the other previously mentioned issues associated with gas engines. It was initially difficult to find optimal configurations for the electric propulsion system. A program called MotoCalc™ made by Capable Computing Inc. was purchased to help optimize the electric propulsion setup. MotoCalc™ works by taking in desired flight characteristics of the aircraft and, using a database of available batteries, motors, and propellers, generates multiple valid configurations. Then the user can examine generated reports about each configuration predicting all performance characteristics, such as time of flight, rate of climb, voltage and amperage at all flight conditions, and component temperatures of the propulsion system.

Several electric configurations using different motors, batteries and propellers were tested in the wind tunnel (Figure 3-7) to compare to MotoCalc predictions. During the tests: thrust, current, voltage, and propeller RPM were recorded at different flow velocities. Thrust was recorded through a load cell attached to the motor mount in the tunnel. Current, voltage, and RPM were recorded by the ESC equipped with data logging. The tests showed that

MotoCalc predictions accurately matched wind tunnel results with enough confidence to guide propulsion component selection.
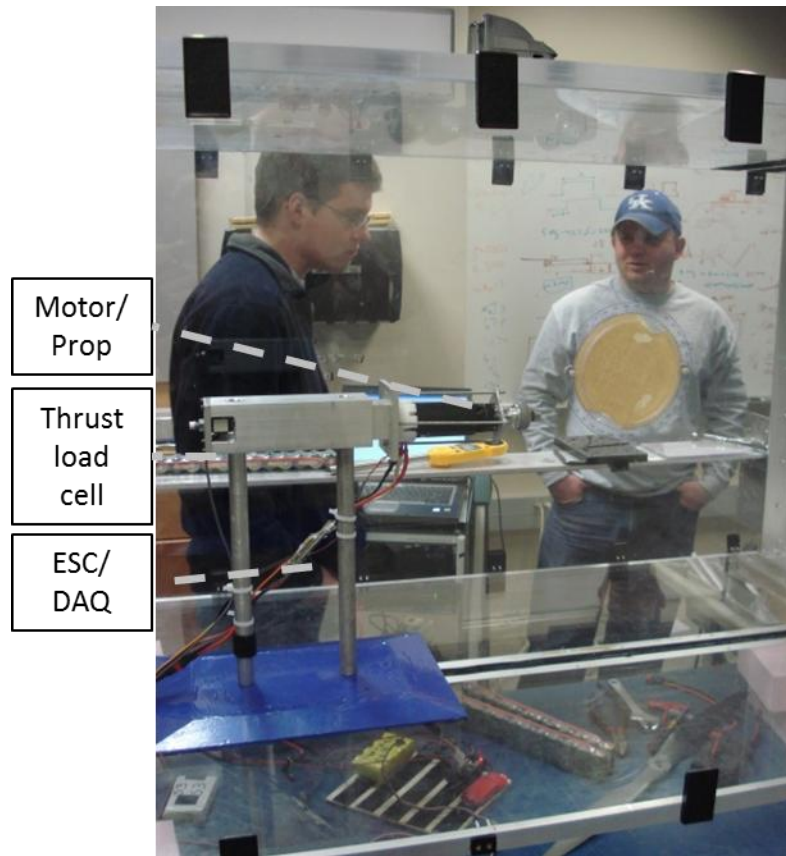
Figure 3-7: Electric propulsion unit being test in UK wind tunnel to confirm MotoCalc predictions

Electric systems, along with the use of MotoCalc™, allow each aircraft to be configured based on its mission requirements by simply running a program and avoids hours of ground testing to predict performance. This expands the abilities of the test bed since different optimal cruising speeds and thrust-to-weight ratios can be achieved. Electric systems also rarely have starting issues and require almost zero maintenance. The typical propulsion system for the test bed is outlined in Section 3.5.

Ultimately an electric system was selected because of the simplicity and adaptability. Glow fuel engines could still be integrated if increased flight time is needed and could still serve as the primary propulsion setup for training new safety pilots due to the extended flight times and quick turnaround time.

3.4   Avionics Selection

26

The avionics for the aircraft need to perform all autonomous flight control and also be capable of recording telemetry for analysis of the wing warping. This includes not only the standard telemetry (GPS, IAS, accelerometer, gyros, and control surface position) but also on-board camera systems for viewing the wing warping. Two systems were considered for the testbed: the Piccolo II™, and ArduPilot™.

3.4.1   Piccolo II Flight Management System

The Piccolo II Flight Management system (Piccolo) as seen in Figure 3-8 is a fully autonomous avionics package manufactured by Cloud Cap Technologies. The Piccolo system has become an industry standard used in many military, law enforcement, and research UAVs. The Piccolo has already been proven to work with the NexStar airframe by work done at the UC-Boulder Research and Engineering Center for Unmanned Vehicles (RECUV) lab using the system to measure atmospheric data and testing aerial networks [40, 38].
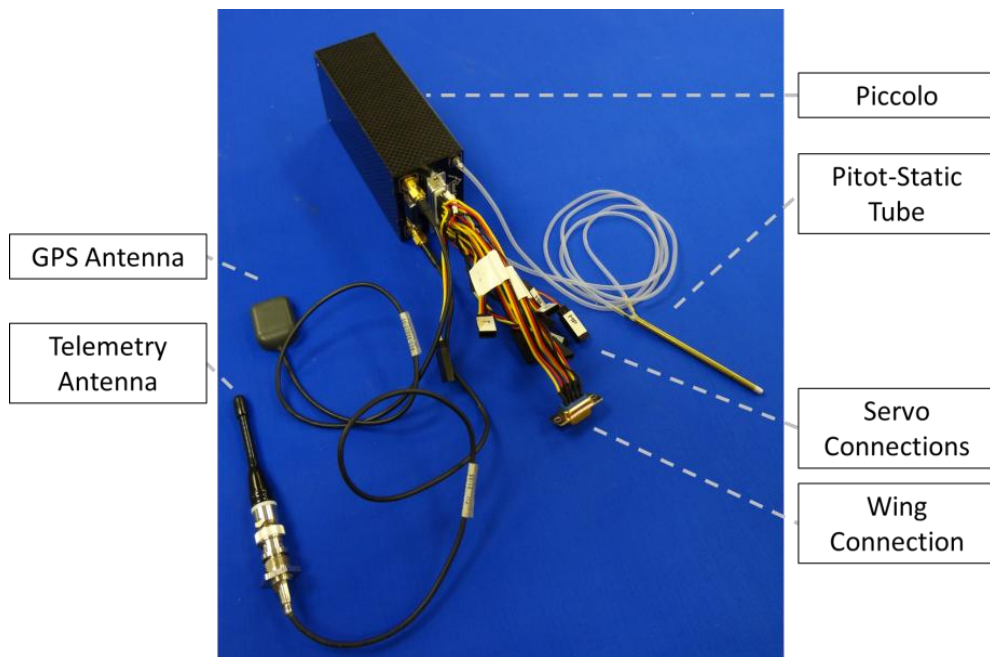
Figure 3-8: Piccolo and components

A full Piccolo system includes the Piccolo autopilot onboard the aircraft and a ground station which handles communications between the laptop, safety pilot, and the aircraft. A full system costs approximately $20k and has a flying weight of 1 lb. The Piccolo records IAS from pitot-static ports, position from GPS and orientation from accelerometers and gyros. The system

also records all control surface positions and system health parameters like signal strength, voltage in, and temperature.

Telemetry is available at a 10Hz rate and is sent over a 900 MHz radio link (Figure 3-9). The same radio sends commands such as waypoint changes and payload control as well as control signals from the safety pilot. The system has full failsafe settings with the UAV set to loiter over a lost communication waypoint until communication can be reestablished.
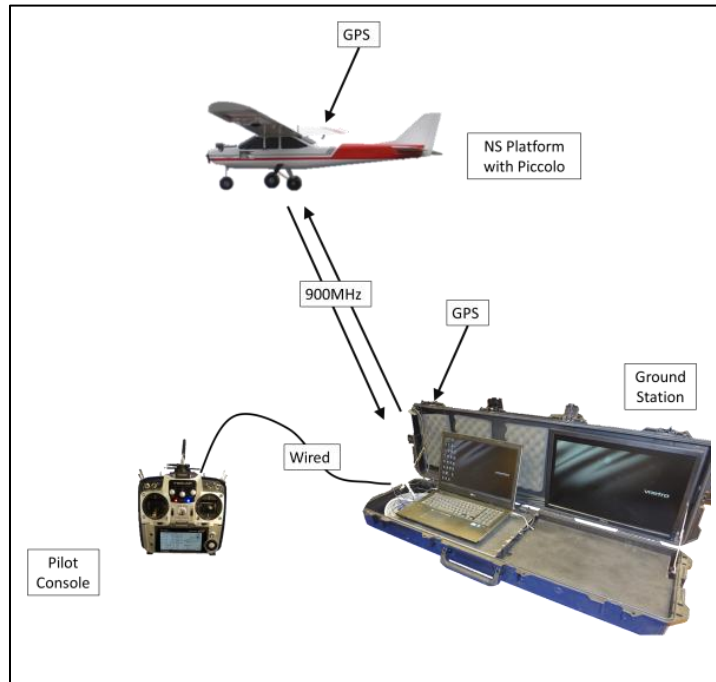
Figure 3-9: Piccolo communication schematic

The pilot's console is wired to the Piccolo ground station (GS) then signals are sent from the GS to the aircraft over the 900MHz telemetry radio. This system has a small lag which can be detected by the pilot but with training is easily manageable [41]. With the testbed described in this chapter, this lag has not been an issue. The lag could potentially be an issue for a highly maneuverable/marginally stable aircraft performing precise maneuvers under RC control. For this application a control switch like the RxMux RC Control Switch™ should be used to switch between the autopilot control and a standard RC receiver on board the aircraft.

Several Piccolo units were available from prior projects and were integrated with the NexStar using guidelines provided by prior use and the RECUV lab. The COTS design of the whole line of Cloud Cap products makes the Piccolo a very robust system with many plug-and-play

options for camera gimbal control and payload interfaces. However the system is closed source without purchasing additional licenses (cost $10k) meaning no changes can be made to the software or control algorithms. While the Piccolo is a proven COTS option, the high cost and weight make it difficult to use in prototype aircraft at higher risk for crashing with tight weight margins.

3.4.2 ArduPilot Open Source Autopilot System

Arduplane™ is an open source autopilot system based around the Arduino™ microcontroller. A community of developers working through DIYDrones.com has been developing the hardware and software since 2009 [4]. ArduPilot™ refers to the flying hardware, while Arduplane is used to reference the project as a whole and also specifically the software. An ArduPilot board can be loaded with different software created by the ArduPlane project such as, ArduCopter, ArduBoat, and others. The board can also be loaded with user created software.

The custom Arduino circuit board called ArduPilot Mega 1.0™ (APM) is equipped with integrated sensors for GPS, barometric altitude, IAS, 3-axis magnetometer, 3-axis gyros, 3-axis accelerometers, laser altimeter, and battery monitor (Figure 3-10). ArduPlane systems cost approximately $500 and have a flying weight of 0.35lbs. The Arduino microcontroller provides all necessary feedback controllers and 2-way radio allows for telemetry to be sent to the ground and commands to be sent to the aircraft.
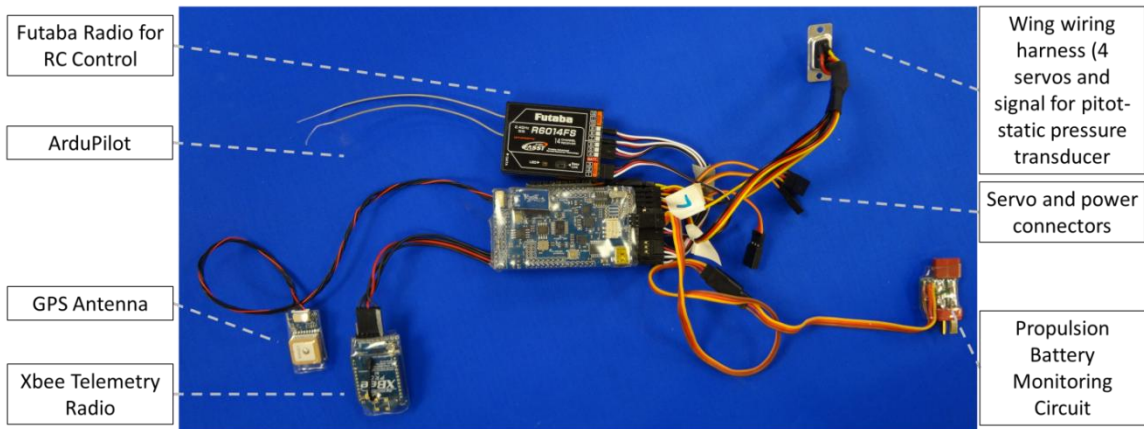
Figure 3-10: ArduPlane APM, Futaba radio and components

Unlike the Piccolo autopilot, the safety pilot's commands are sent from a standard RC transmitter directly to a RC receiver in the aircraft and into the APM (Figure 3-11). One channel

of the radio is used to control whether the APM will operate in fully autonomous, stabilization, or manual mode. The ArduPlane is capable of multiple levels of stabilization that fall between direct manual control and fully autonomous operation. Telemetry is recorded at rates varying from 8Hz to 50Hz depending on the radio setup.
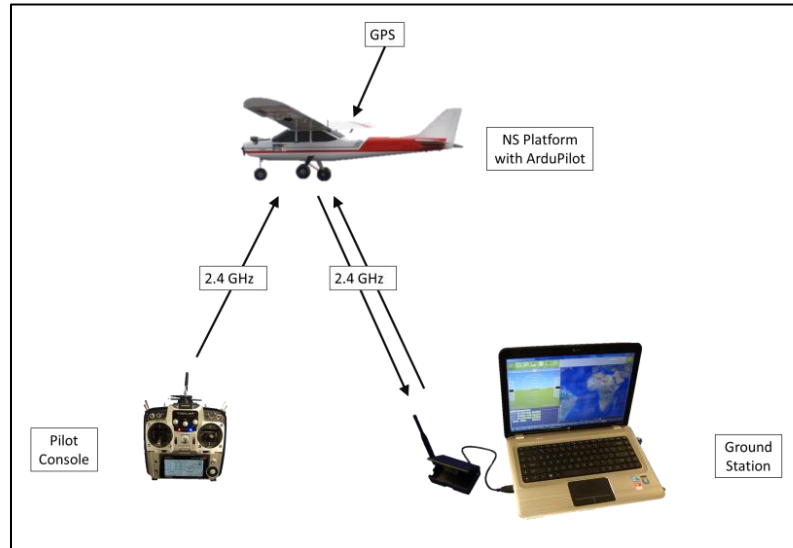
Figure 3-11: ArduPlane communication schematic

The open source of the ArduPlane allows for complete customization of all parts of the code. This also means that the system can often have bugs and difficulty integrating sensors. An active community of developers at DIYdrones.com is continuously updating and addressing problems. The low cost and weight of the APM make it ideal for testing prototype aircraft that are at a higher risk of crashing.

3.5   Typical Test Bed Configuration Specs

Following are the specifications of the general setup of the testbed aircraft. This configuration has been the primary configuration used in the lab for various tests. It is important to note that this platform has been designed to easily change the avionics package and propulsion system depending on mission requirements. The most common configuration's performance specifications are outline in Table 3-1.

Currently at UK the NS platforms have flown over 6 hours with 5 hours of autonomous flight and over 50 landings with 10 autonomous landings. They have been used as an aerial

camera platform for 3D scene generation (Figure 3-12) and will be used in future projects supporting aerial networks and atmospheric boundary layer measurements.

Figure 3-12: Left) NS platform in flight Right) Onboard camera view from one NS platform viewing another

Table 3-1: Performance and specifications for typical NS platform configuration

NS Platform Standard Configuration	
Airframe:	
Span	69 in.
Length	56 in.
Chord	10.5 in
GTOW (empty)	8 lbs.
W/S (empty)	25 oz/ft^2
Propulsion:	
Motor	RimFire 50-55-500
kV	500
Power	1100W
ESC	Castle Creation 45Amp ESC w/data logging
Batteries	Two 3300 mAh 4s 65C LiPo in series
Performance:	
Range	Radio 1.5 mi, operations limited to line of sight
Endurance	35 min.
Payload	5 lbs. (max)
Cruise Velocity	35 kts
Dash Velocity	50 kts

The development of this platform is the result of 20 test flights and months of work. It often takes several attempts during development before achieving a successful flight. Sometime this means the loss of the airframe in a crash, but more often this means a problem was

31

discovered on the ground and no flight was attempted. The UK UAV Lab has developed a strictly enforced series of checklists for each aircraft and ground component. A system of flight tagging airframes, batteries, and ground components once check out is complete has been developed. Checklists also include post flight procedures which insure that necessary maintenance and changes are made between flight tests. This system has cut the number of failed flight attempts between successful flights in half.

All autonomous flight testing takes place at the Lexington Model Airplane Club (LMAC), an Academy of Model Aeronautics (AMA) chartered site. Flights followed the guidelines listed in the AMA Manually Controllable Programmed Outdoor Model Flight Operations document [42]. These guidelines include limiting operations to line-of-sight and within the chartered clubs' flying area. An AMA pilot must always be able to take manual control of the aircraft. Aircraft must first perform a full flight under manual control before attempting autonomous flight. Flight speeds are limited to 60 mph. The aircraft and pilot must meet/abide by the AMA safety code [43].

4   WARPING WING DESIGN

Several approaches to designing an inflatable warping wing were considered. The first was the modification of a current inflatable wing to warping wing. But this comes with many complications and could destroy an expensive custom-made wing. A second option was to develop the manufacturing techniques in house to make inflatable wings. But previous attempts at UK have shown there to be many variables in the process that are not well understood and require special equipment. Working with ILC Dover or other companies already capable of manufacturing inflatable wings could yield a high quality warping inflatable. But, for this to be cost and time effective, there would need to be confidence in the design to not only fly but be able to be integrated with the autopilot.

An intermediate prototyping step needed to be developed to allow potential warping designs to be tested and modified quickly and cost effectively. The main complication working with the inflatables is being able to modify and seal them. An inflatable analog having the same structural characteristics could be used to test wing warping. Once a design is proven the analog can be replaced with an inflatable structure.

4.1   Overview

Using foam in place of an inflatable surface a warping design was created using the twist actuation outlined in Section 2.2 and a rigid spar. The twist mechanism was selected for testing first since it was one of the simpler methods to create a mechanism for and can effect changes over a large portion of the wing. The mechanism was completely internal decreasing the drag compared to an external mechanism. A torque tube was passed through the foam and acted as both the spar and the actuation. The wingtip of the foam was attached to a rigid rib secured to the torque tube. The inboard rib was fixed in place while the outboard was rotated by the torque tube, warping the wing (Figure 4-1).
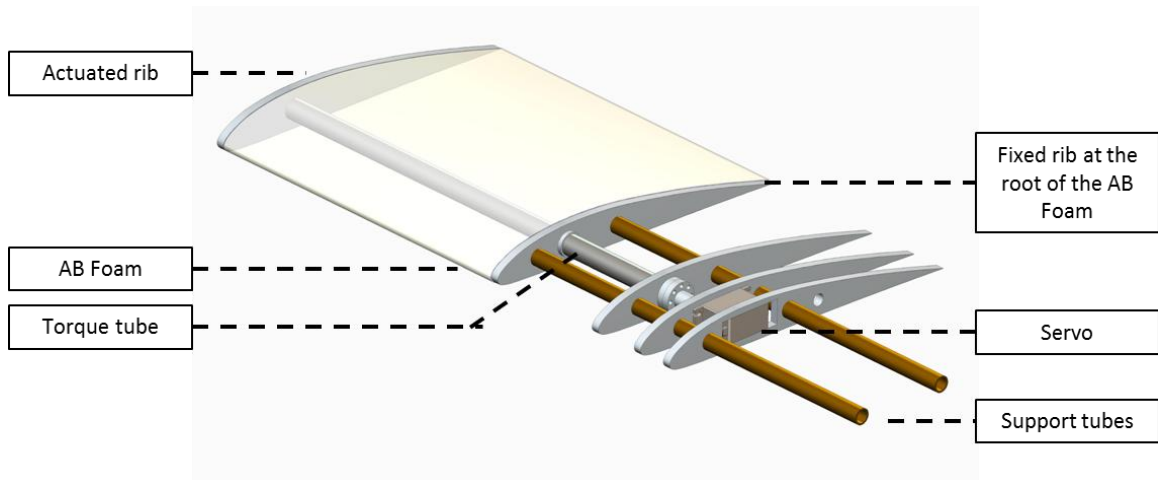
Figure 4-1: Twisting mechanism labeled drawing (carbon fiber skin over mechanism not shown)

The design of the wing also allows for warping sections to be quickly changed to facilitate testing. Using foam as an analog for inflatables allows for later testing of mechanisms for camber control and other potential methods. In the following sections each component will be detailed.

4.2   Deformable Material Selection

The deformable material for an inflatable analog must match the mechanical properties of existing inflatable structures and also be able to be manufactured quickly and easily. Several foam materials were considered and available material properties were examined. Due to the wide range of properties given even when marketed under the same name or type, it was decided to purchase several foams and perform qualitative tests. Several foams were purchased and tested for torsional stiffness and manufacturability. Some foams were immediately determined not to be viable due to being overly stiff or overly soft. Other foams' cell structures would break down after only a few bending cycles and not return to its original shape.

It was important that the foam selected be able to be manufactured easily to the desired shape. This meant that the foam would have an accurate shape once complete and smooth surface finish with relatively low permeability. The torque tube which will actuate the wing is internal so the foam must be able to be manufactured with voids. Eventually the twisting mechanism will ideally be the entire wing. This means that it was not feasible to bore an accurate hole for the torque tube.

The first foam tested was Slow-Recovery Polyurethane foam (Figure 4-2 A) commonly called memory foam or Confor™. The initial feel of the foam indicated that it was adequately stiff and the surface finish from the factory was acceptable. The foam is open cell, meaning that the surface is permeable but not enough to completely rule it out as an option. The green version selected was the highest density at 5.8 lb/ft^3 but this also meant it was the stiffest.

Figure 4-2: Foams tested: A) polyurethane, B) high density polyethylene, C) low density polyethylene, D) AB Foam

Using a foam hot-wire cutter a small section of foam was cut to the shape of a wing. For installation of the torque tube, a slot and circular hole were cut into the foam with the hot wire. Later, adhesive was used to close the slot. Wood ribs were bonded to the ends of the wing and the torque tube was installed. The TE was replaced with balsa wood because it was too weak and would deflect even under gravity loading (Figure 4-3). The hot wire cutting method worked easily for the exterior shape but was difficult and inaccurate for cutting the torque tube hole. The hot wire actually improved the surface finish and permeability as it melted the outer surface, sealing some of the open cells in the foam (Figure 4-4).
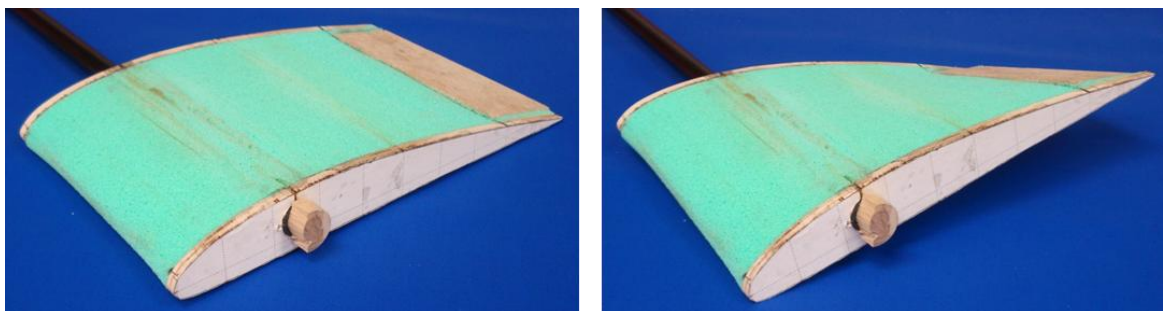
Figure 4-3: Mockup warping wing made from hot wire cut polyurethane foam

Figure 4-4: Surface quality of foams tested

Even with the modified TE, the wing was still not stiff enough even for the short test span. In addition, the polyurethane foam's stiffness is based on the rate of deformation. Meaning that as the foam sits at rest, it slowly deforms under its own weight. This, combined with the weight of the foam, meant that other foams had to be considered.

A test section of foam was machined using a 3-axis mill and found to machine very well with a surface nearly equal that of the factory finish. But this was not explored further at the time since the mill could only cut the outer surfaces and not the opening for the torque tube. Later a method was developed to machine the foam, and tested on the polyethylene foam and is discussed below.

Figure 4-5: Black and blue polyethylene foams

Polyethylene foam was chosen for testing because of low density. Two densities were selected a black 2.2 lb/ft^3 and blue 1.8 lb/ft^3 (Figure 4-5). Both densities of foam have a very open cell structure meaning foam has a rough permeable surface. In order to be a viable option, the foam needs to be skinned with a fabric to maintain proper flow around the wing and not have the flow permeate into the surface. The foam did not cut well with a hot wire so a method to machine the foam was developed.

Since a 3-axis mill is unable to mill the torque tube hole, the CAD model of the foam airfoil was split along the camber line. The wing would be machined in two parts (top and bottom surface) and then bonded. First the outer surface of either the top or bottom of the wing is milled. Then the part is flipped into a cradle which has the negative shape of the outer surface in it to support the part. The inside surface, which is the camber line, is milled on the back side and one half of the circular hole for the torque tube is milled (Figure 4-6). When the top and bottom are joined along the camber line a perfect circular opening is left for the torque tube (Figure 4-7).
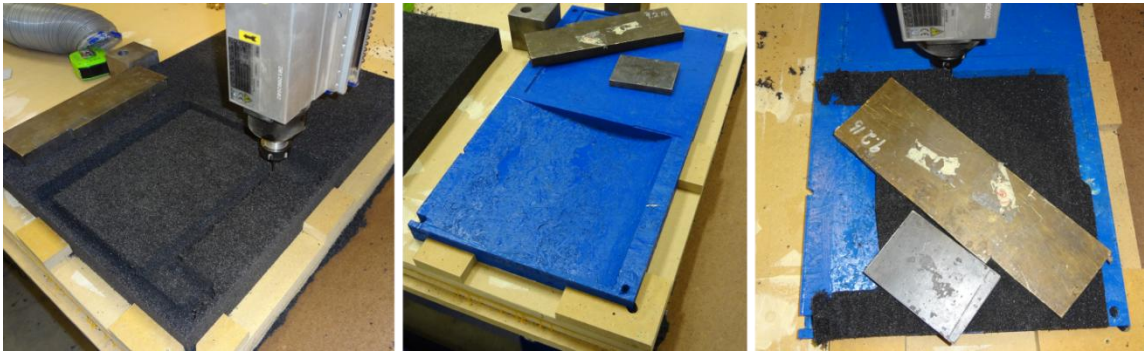
Figure 4-6: Series of images showing the camber line milling flip job
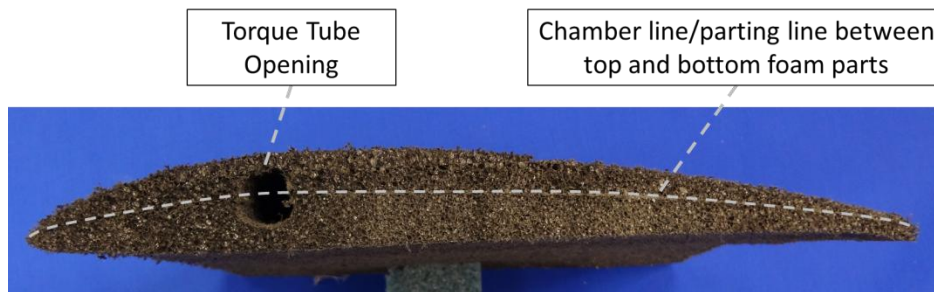
Figure 4-7: Foam halves joined at chamber line

This method was tested on both polyurethane and polyethylene foams. For the polyurethane the machining produced highly accurate outer and inner surfaces. The polyethylene surface due to its large cell structure, was left very rough. The machining bit made small tears in the polyethylene foam. Instead of a smooth cut, little slivers of foam left the surface almost furry. The machining was time consuming and, due to the thin TE the foam was often grabbed and torn by the spindle ruining that piece of foam and requiring the process to be restarted.

Due to the surface roughness of the milled polyethylene foam, Spandura™ fabric was selected to skin the foam. The Spandura fabric was selected because it was shown to wrinkle the least under actuation of the fabrics considered. Cylinders of fabric were sewn and then rolled over the foam wings. The ends were bonded with 5-minute epoxy (Figure 4-8).

Figure 4-8: Black foam wings with fabric skinned being applied

While the polyethylene foam was initially able to be warped by the servos, the addition of the fabric increased the torsional stiffness beyond the servos' limits. A complete discussion of the design of the warping actuation is in Section 4.5.

The issue for the foams was finding a balance between being stiff enough to maintain shape, yet having a low enough torsional stiffness to be actuated. Machining the foam from the rectangular shape to the airfoil shape also led to difficulties resulting in inaccurate parts with poor surface finish. It is possible that by adding additional voids in the foam, and changing the machining bits, these issues could be fixed. But another option was considered.

The final option considered was two-part urethane pour foam, often called AB foam. Instead of the foam arriving as a block and machining to shape, AB foam works by mixing two liquids together starting a chemical reaction that makes the liquid rapidly expand and harden. The foam selected was FlexFoam-IT! III™ sold by Smooth-On Inc. Unlike other urethane AB foams, this foam does not become rigid when cured. With a $3lb/ft^3$ density, the foam fall between the foams already discussed.

Using a 3-axis CNC, a four-piece female mold was made for the top and bottom surface with two end caps to be the mold ends. The molds for AB foam do not require the high quality surface finish of gelcoat like those detailed in Section 4.4. As a result the mold was able to be milled directly into plywood plugs and then primed and sanded. AB foam is not compatible with

the PVA release agent typically used during layup to help parts release from the mold. Instead a thick layer of mold wax is applied (Figure 4-9).

Figure 4-9: A) Four part mold and torque tube B) Mold being waxed for pour

The molds are also required to have openings to allow the AB foam to expand. If the openings are too small, pressure will build in the mold keeping the foam from properly forming. The cell structure collapses and turns to a rigid, highly dense material. If the openings are too large, the foam will not build up enough pressure to be forced into the entire mold resulting in voids in the final part. After experimentation with small sample molds, the openings were placed at the TE of the top surface mold in the form of two small slits cut into the mold flange (Figure 4-10).
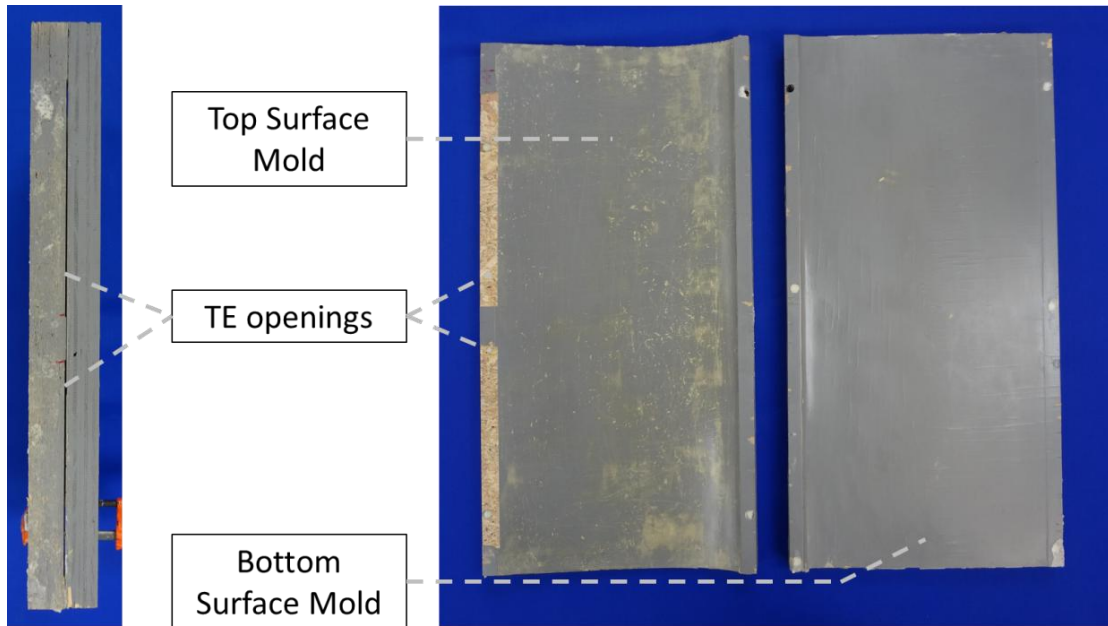
Figure 4-10: AB foam mold

To make an AB foam wing, the molds are prepped with wax and all materials and supplies laid out ahead of time due to the quick cure of the foam. The following process can be seen in Figure 4-11. The two parts are mixed together for 30 seconds. Early attempts showed that getting the two parts mixed at the correct ratio and thoroughly mixed is vital to the foam properly curing. At 30 seconds the foam begins expanding and must be poured into the mold and the mold aligned and clamped. After two hours the part can be removed flashing trimmed and torque tube freed.

Figure 4-11: Manufacturing AB foam wing

The mold makes a 21 inch (2 chord length) part (Figure 4-12). The part can easily be cut to shorter lengths. The choice was made to move forward using the AB foam for the deformable wing because it produced the most accurate part with acceptable torsional stiffness and smooth surface finish. It is also the easiest to manufacture once issues with mold release and size of the openings were solved. Some concern was raised with the relatively flexible TE. This issue is later addressed in Chapter 5.
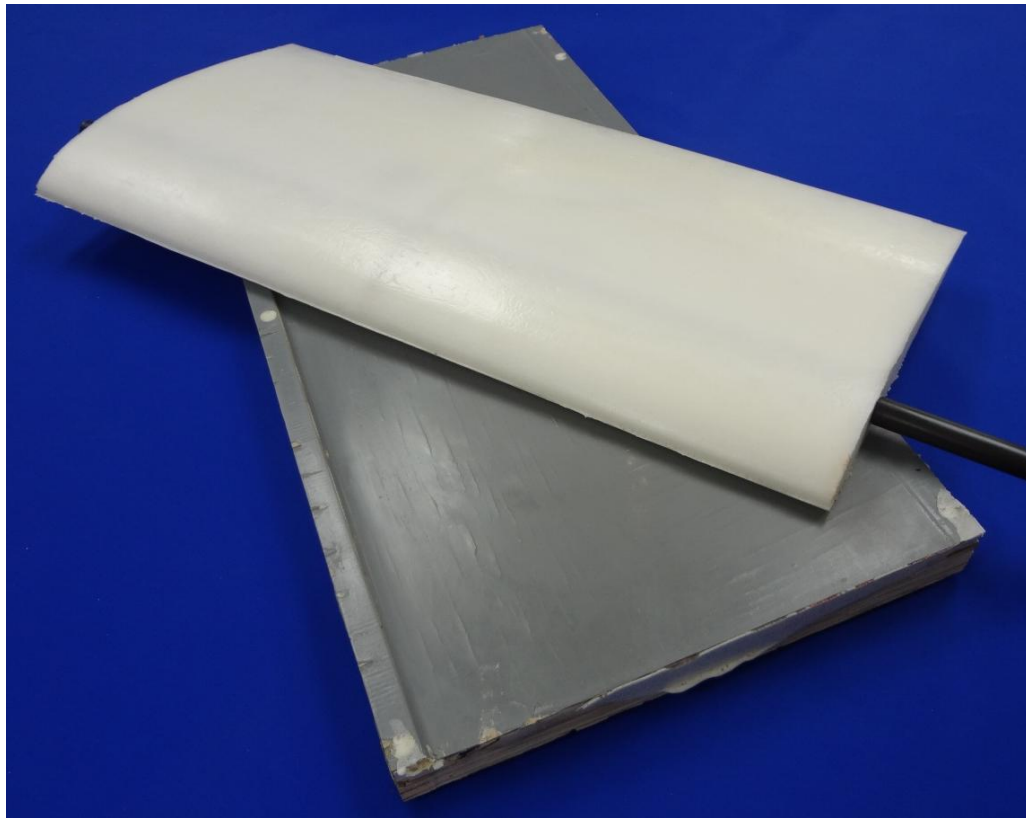
4.3   Overall Wing Design Requirements

The wing being designed for flight testing needed to meet several requirements. It had be able to work with the existing NS platform. This governed the general size and weight of the wing. The wing needed to be constructed to accommodate design changes. The wing also needed to be equipped with conventional ailerons which can be used as a safety measure in the event that the warping actuation is not controllable. They will also be used during takeoff until a safe altitude for testing is reached.

The wing was designed to have a center section with conventional aileron mounted to the fuselage. Interchangeable outboard sections were designed for the warping actuation. This allows for testing of different designs with reduced cost and construction time.

Figure 4-13: Wing warping wing and standard configuration wing on NexStar test bed

The stock NexStar wing was used as the starting point, with a chord length was set at 10.5in and the span at 70in. The dihedral in the stock wing was removed to make construction easier and to allow for a more responsive aircraft in roll. Due to the high-wing design of the airframe, the aircraft was inherently stable in roll. A comparison of the two wings can be seen Figure 4-13.

The airfoil selected was a USA-35B which was thought to be the airfoil used in the existing wings. It was later discovered that the airfoil used by Hobbico to make the NexStar is actually a modified form of the USA-35B (Figure 4-14). Athena Vortex Lattice (AVL) models were run with the USA-35B and predicted that there was enough lift and the aircraft was controllable without needing changes to the airframe [44].
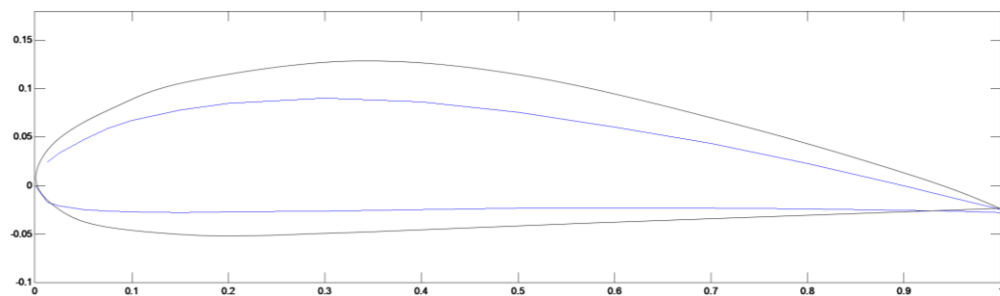
Figure 4-14: USA-35B airfoil (blue) compared to the stock NexStar airfoil (black)

4.4 Center Wing Section Design and Manufacturing

The center wing portion was sized to use the smallest span (to maximize the amount of span used for wing warping), but still large enough to have the conventional backup ailerons

provide sufficient roll authority. This is an important feature that allows the aircraft to fly without using the warping actuation. This addresses contingencies of warping mechanism failure, unpredicted control issues with wing warping, or both ailerons and warping can be used if the warping does not provide enough authority still allowing some data to be collected. The ailerons can also act as flaps.

Using a historically-based aileron sizing chart (Figure 4-15) from Raymer [45], and limiting the aileron to 25% of the chord due to servo placement in the wing, the smallest span the ailerons can be is 0.3 times the span of the wing. The planned span of the wing is 70 in meaning a minimum of 20 in (10 in per semi-span) are necessary. Due to the ailerons being placed at the root instead of nearer the tip, as is typical, the ailerons were increased to 15 in for each semi-span making the center section span 35 in after accommodating the fuselage width.
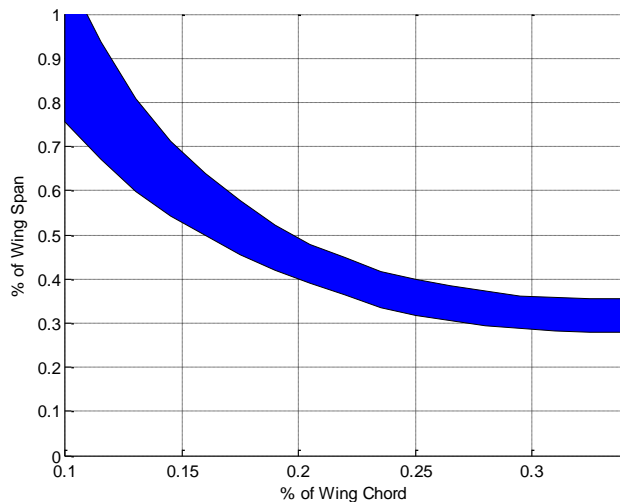
Figure 4-15: Aileron sizing chart adapted from Raymer [45]

It was decided to construct the center wing section with carbon fiber, balsa, fiber glass, and resin composite because of the relatively high stiffness and light weight construction. A typical stick-built/MonoKote™ method used to make the stock NexStar wing would not be ideal for this design because of the increased weight of the airframe and the structural connection between the center and warping sections.

The techniques below are a combination of those learned through reading texts, following an active online community of composite aircraft builders, and engaging in discussions with

faculty and students at Oklahoma State University's Mechanical and Aerospace Engineering Department [46, 47, 48].

The male plugs for the top and bottom surface of the wing were cut out of medium dentistry fiberboard (MDF) on a 3-axis CNC. The plugs then went through a series of painting and hand sanding. The machining marks are first sanded out of the MDF starting with 100 grit sandpaper and finishing with 220 grit sandpaper. Any spots below the intended shape were filled with automotive body filler. The mold was then sprayed with automotive primer and dry sanded with 220 grit sandpaper. A final coat of primer was then sprayed and the sanding began with 220 grit dry sandpaper and was increased until 1500 grit wet sanding finish was achieved (Figure 4-16).
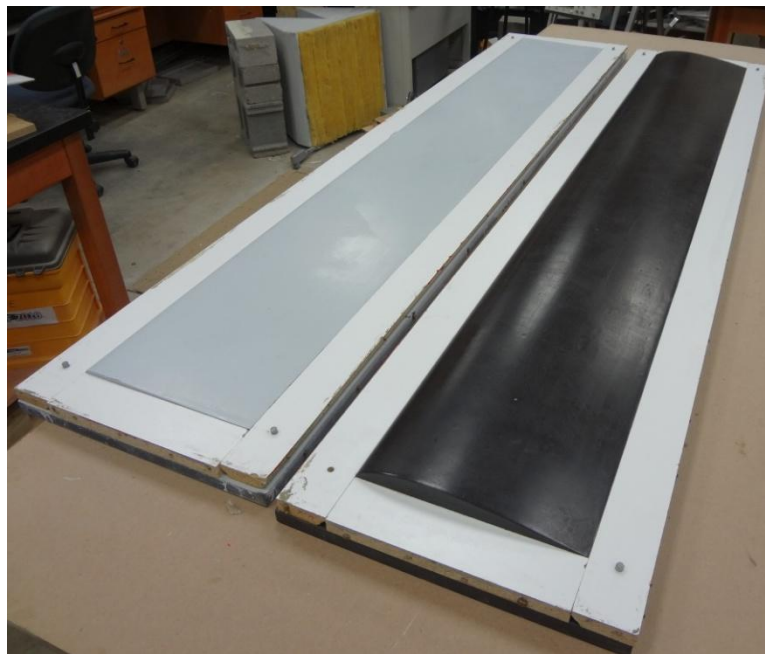
Figure 4-16: Male plugs ready for gelcoat, black top surface, gray bottom surface

Despite that the center section was only 35 in span, a full 70 in span mold was created. The center section was laid in the middle of the mold and trimmed to final dimension. A full span mold was also created to accommodate the potential need to increase the span of the center section without needing to construct a new mold. In addition, it was planned to construct a full span wing with conventional ailerons as a direct comparison to wing warping. Due to time constraints this wing was constructed but not flown prior to the completion of this thesis.

From the male plugs, female molds were made using gelcoat and fiber glass. Gelcoat mimics the plug's surface and provided a durable long lasting surface for part production (Figure 4-17).

Figure 4-17: Female molds constructed of orange gelcoat and fiberglass

Both molds were waxed and prepped with PVA release agent. A typical molded composite process was followed to construct the wing center section. Each layer is wetted out with resin before being placed. The first layer, which makes up the outer surface of the wing, is 5.7oz/yd^2 carbon fiber laid at 0°/90°, meaning fibers are aligned in the span and chord-wise directions. A Kevlar strip is laid on the bottom surface hinge line of the ailerons. Once the surfaces are joined this Kevlar will be the aileron hinge. 1/16" balsa is then laid to provide skin stiffness. Gaps are left in the balsa over the aileron hinge line and at the quarter chord. In the quarter cord balsa gap, carbon fiber tow is laid in the span direction as the compression and tension layers of the main wing spar. Each wing is then covered in a 3oz/yd^3 structural fiber glass laid at a 45° bias. Each surface is covered in peel-ply fabric which gives the inner fiberglass surface a rough finish for structural bonding. The peel-ply is removed after the parts' are cured. Each surface is then prepped for vacuum bagging which is used to remove excess resin and hold the part's shape during curing.

Once cured, the peel-ply is removed with warm soap and water. The edges are trimmed on each surface flush with the parting lines of the mold in preparation for bonding the two surfaces together. The molds are again waxed and PVA applied. The internal structure of the spar's shear web and carbon fiber sleeves for warping wing attachment are bonded to the top surface

(Figure 4-18). The carbon fiber sleeves were run the entire span for simplicity and to aide in rib alignment despite only being needed between the outboard two ribs for mating with the warping inserts. This resulted in a very stiff final part. CNC cut composite wood ribs are used to align parts. A total of six ribs were used. The outboard pair provide the mating surface to the warping sections. The next pair in supports the end of the rods from the warping inserts once installed. The inner most pair of ribs is placed to help distribute the load of the forward and aft mounting bolts at the center of the wing. A combination of epoxy resin and colloidal silica forms a thick structural adhesive which is applied on any surface that will bond the top and bottom surfaces. The two molds are aligned face to face and clamped together while the wing cures (Figure 4-19).
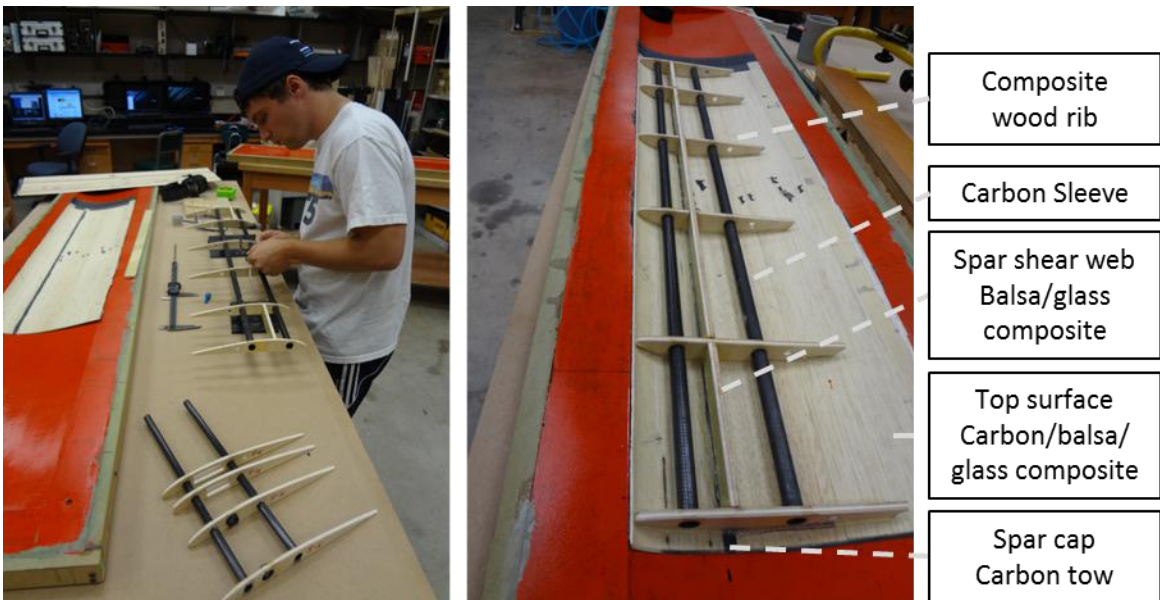
Figure 4-18: Installation of shear web and carbon fiber sleeves for holding wing inserts
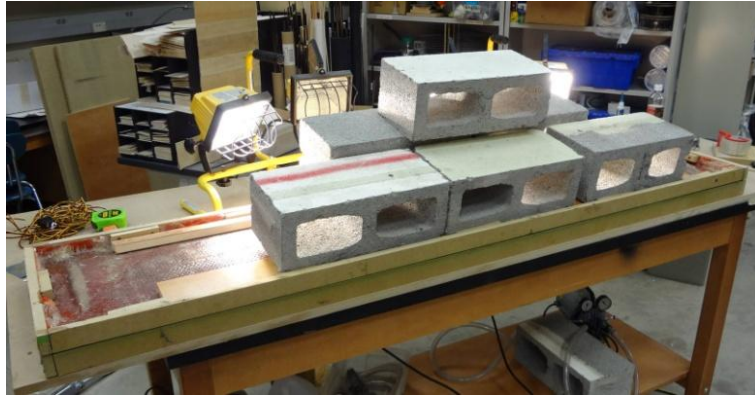
Figure 4-19: Wing surfaces being joined

Once the wing is removed from the mold the ailerons are cut and the carbon over the Kevlar hinge scored. Wipers are installed to close the gap created when the ailerons deflect (Figure 4-20). Servos are installed inside the wing with all internal linkages (Figure 4-21). A pitot-static tube and pressure transducer were installed in the wing (Figure 4-22). All wiring for the two aileron servos, two warping servos, and pitot-static pressure sensor are installed and run through a single 9-pin serial plug.
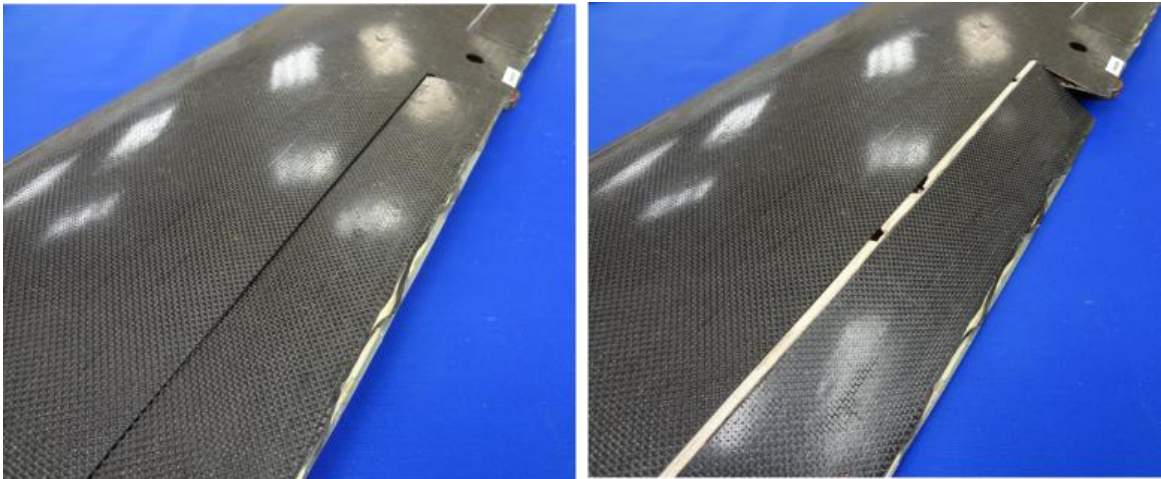
Figure 4-20: Wipers installed on ailerons
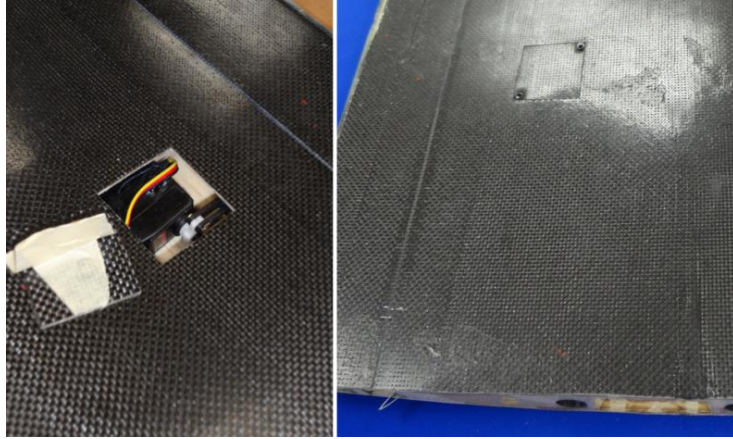
Figure 4-21: Servo and linkage install

Figure 4-22: Pressure transducer and pitot-static tube

4.5   Warping Inserts

Each warping insert is designed to operate independently from the center wing. The only interface between the insert and the center wing is the carbon fiber tube and sleeve to carry structural loads and the servo signal and power. This also allowed the insert to be tested separately from the aircraft.

The insert is a hand-built assembly consisting of two carbon fiber support rods that connect the insert to the center wing, several CNC cut composite wood ribs, servos, torque tube, carbon fiber skins and the deformable foam (Figure 4-23). This design allows identical parts to be assembled with different length carbon fiber rods to achieve different span length warping sections. The carbon fiber skin gives the structure the necessary torsional stiffness when the warping servo is actuated. All bonding for the inserts is done with 5-minute epoxy.
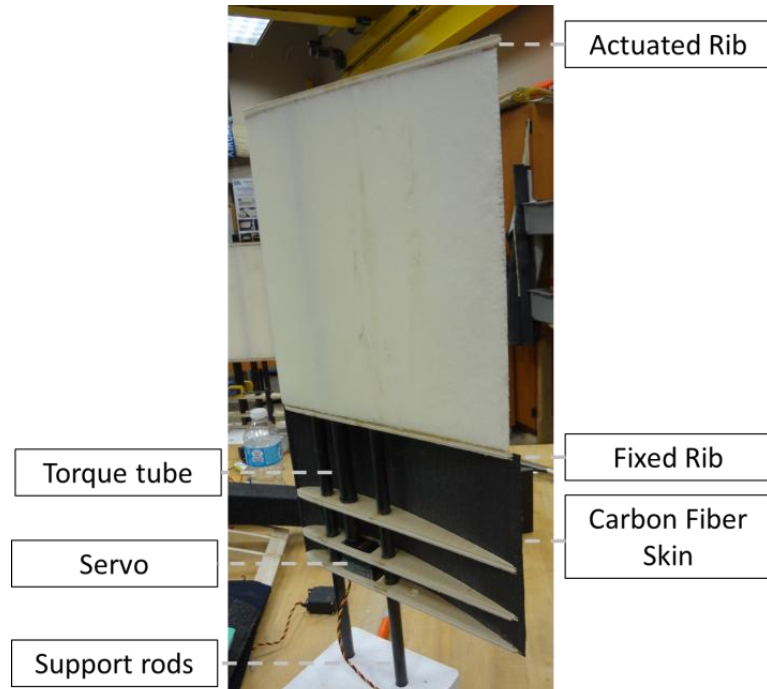
Figure 4-23: Complete warping insert with bottom skin removed

The use of mandrel-wrapped carbon fiber sleeves with high tolerance ID in the center wing and pultruded carbon fiber rods with high tolerance OD and CNC cut ribs for spacing proved to provide a consistent no-slop connection between the inserts and the center wing section.

The servos used for warping were Hi-Tech HS-5995 digital servos with 333oz-in of torque. This is the highest torque servo available in this size. The servo can rotate ±45° and consumes 3 amps at 5V at stall torque. The complete wing with warping inserts weighed 3.7lb, compared to the stock NS platform wing weight of 2.2lb. The wing was tested for strength by lifting the flight ready aircraft by the wing tips simulating a 2g loading case. Little to no deflection was seen.

5   TRUCK TESTING OF WARPING WINGS

The completed wing was mounted on the fuselage. In preparation for flight testing, a hop test was performed (Figure 5-1). A hop test starts with a series of increasingly fast taxis. Eventually the aircraft is able to rotate and lift off the ground briefly before being set back down. Typically this last a couple of seconds and the aircraft reaches one to two feet above the ground.
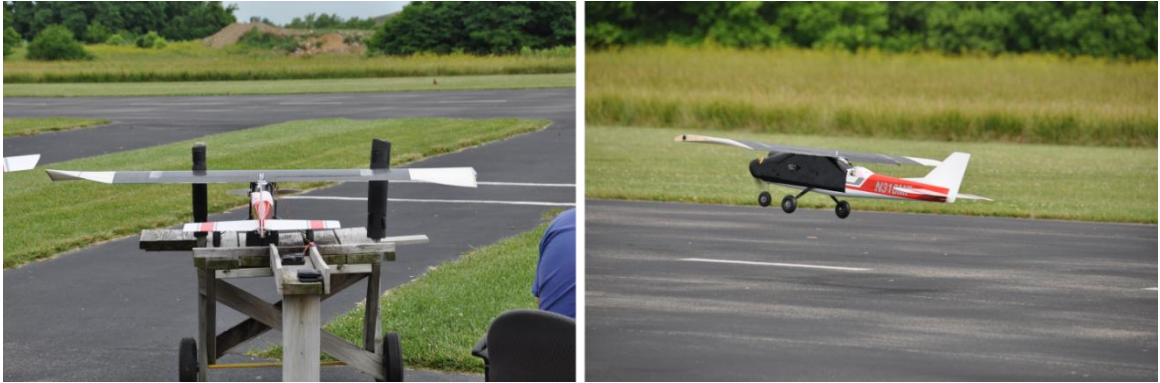
Figure 5-1: Completed wing hop testing

During this brief time in flight, it was observed by ground crew and confirmed by an onboard camera that the TE of the wing was beginning to oscillate (Figure 5-2).
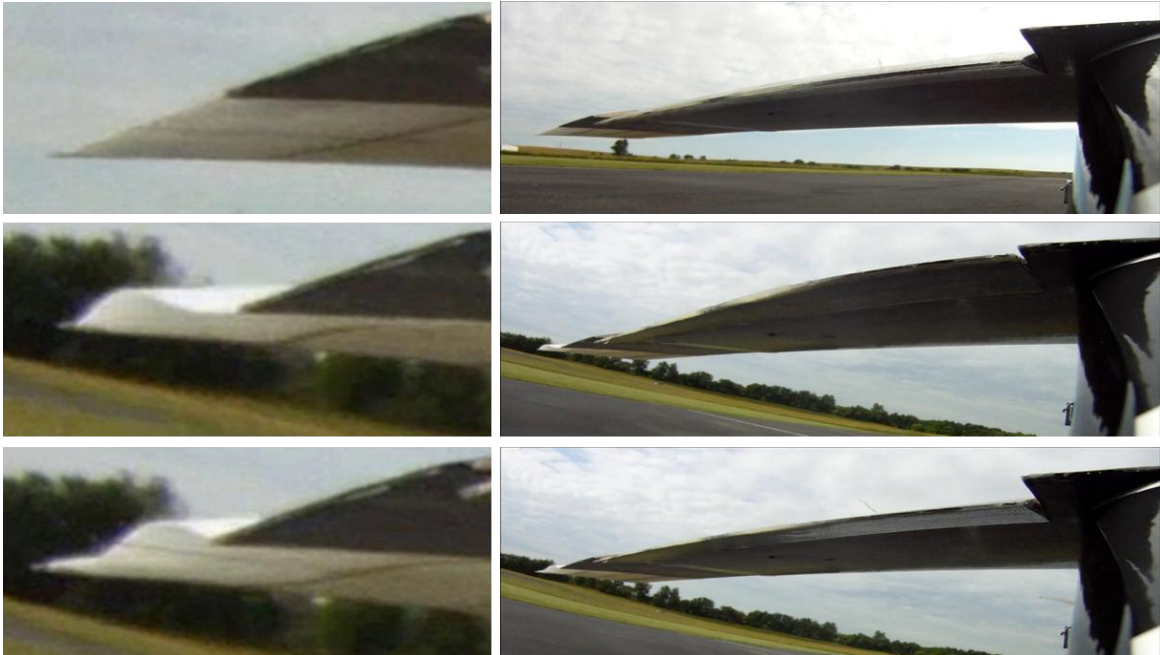
Figure 5-2: On board camera showing TE oscillation during hop test

It was decided before flight testing could continue that another way of testing the wings would need to be implemented to better understand these oscillations.

Previous work done by Loh and Kehoe [19, 49] showed that using a vehicle in place of a wind tunnel provided by a quick method for testing components that could not be tested in a wind tunnel. The only wind tunnel at The University of Kentucky able to fit the warping section of the wing was, throughout this time period, being used by another project and could not be reconfigured for this test. While the flow above a moving vehicle would not be as ideal as in a wind tunnel, the purpose of this test is to get a rough idea of the behavior of the wing under aerodynamic loads.

5.1   Truck Setup

The wing inserts were removed from the center portion of the wing for testing. They were mounted vertically so that flow potentially traveling vertically off the cab of the truck would move across the wing in the span direction and not cause a false measurement of AOA that could result if the wing was mounted horizontally. This orientation also allowed the entire surface to be easily viewed by cameras. See Figure 5-3 below. A wood structure was assembled to hold the wing well above the cab of the pickup. The wing is mounted with a zero angle of attack.

Figure 5-3: Structure secured in pickup truck

The primary instrumentation for this test was cameras used to view the wing deformations during the tests. Two cameras were mounted with suction cups to the truck's body and can easily be moved to view different parts of the wing. Each camera is a GoPro High Definition (HD) recording at 30Hz and 1080p resolution. Video is recorded in each camera and a live feed was available on a monitor in the cab. See Figure 5-4 below. The Arduplane system outlined in Section 3.4.2 was used to record servo position, GPS, and IAS. The ground station is located in the cab and monitored during the tests. A digital multimeter was also installed to measure the electrical current powering the servo. This will give some insight to the loads being placed on the servo and will indicate whether a larger servo is necessary for flight.

Figure 5-4: Instrumentation in truck to monitor telemetry systems and camera feeds

For the first runs tufts of small green yarn were attached to the wing. This was done to confirm that the flow is running perpendicular to the wing and behaving predictably. See Figure 5-5 below.

Figure 5-5: Tufts on wing to confirm flow direction

5.2 Results from AB Foam V1

The first wing tested was the starboard wing insert that was used during the hop test. Several runs were done at speeds from 25 to 45mph. The full range of deflections was also tested. See Figure 5-6 below.

Figure 5-6: Images from cameras during truck testing

Initially the cameras were focused mainly on the TE edge looking for oscillations. It was quickly realized that while the observed oscillation was there it did not grow significantly with speed. Further testing of the port wing and later versions of modified wings all showed the TE oscillations to be minimal and not divergent with increasing speed.

It was observed early on that the LE of the wing deformed downward (Figure 5-7). The deformation was proportional to speed and present at all deflections. Testing was capped at 45 mph to prevent possible damage to the foam.
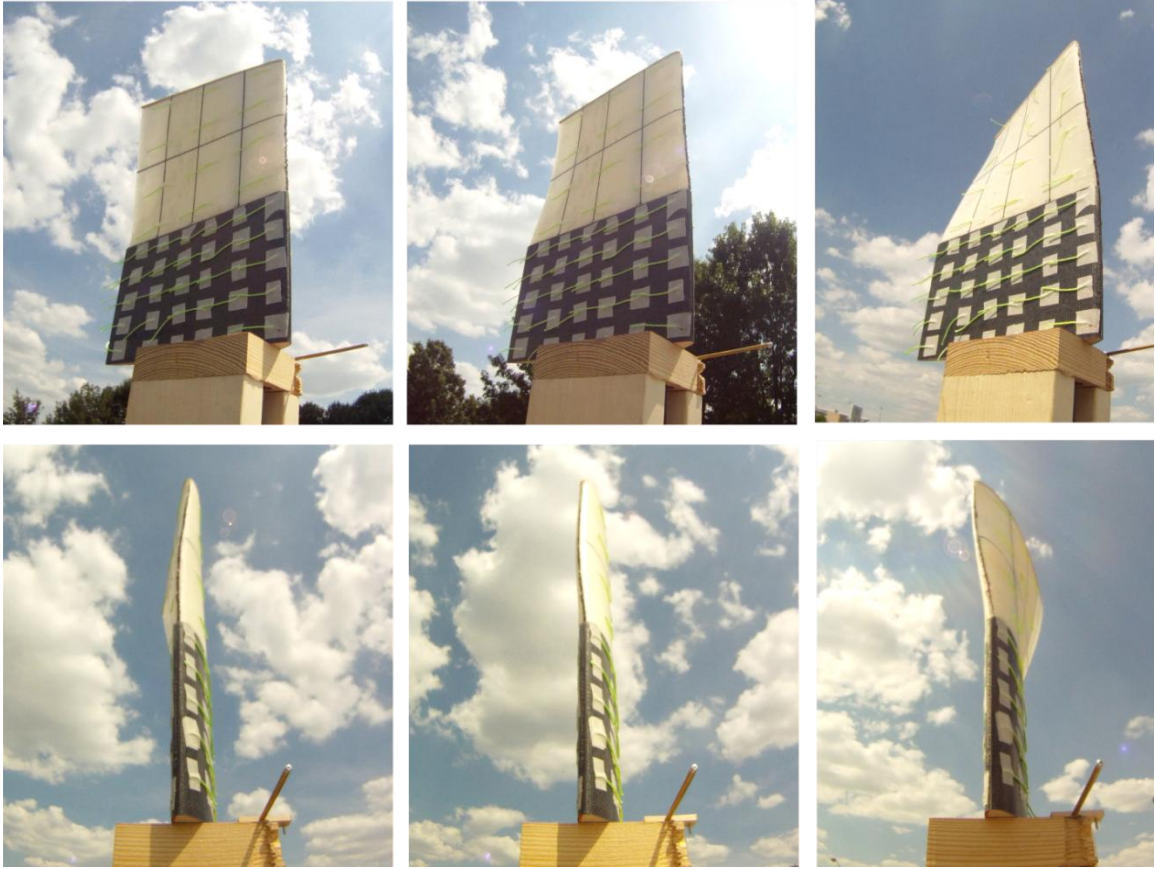
Figure 5-7: ABv1 foam at 40 mph with negative, zero, and positive deflection all showing LE deformation

The deformation seen in Figure 5-7 at the center portion of the wing is the result in the change of the cross section of the wing and not a simple rotation about the torque tube. The difference is illustrated in Figure 5-8.
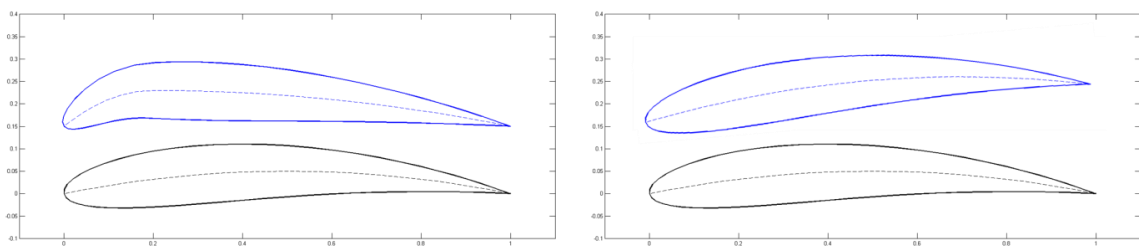
Figure 5-8: Deformation of the center of the wing vs. simple rotation

During initial sizing of the wing models, it was decided to start with a small portion of the span. If the distance between the fixed root rib and the outboard actuated rib was too great, or the material too soft, the center of the wing would rotate around the torque tube

uncontrollably and independently of the ribs. In this case the actuated and fixed ribs were still applying enough force at the center to maintain control of the center section but the foam is deforming due to aerodynamic loading. The deformation meant that the center not only had a decreased AoA but also an increased camber.

The flow was forcing the portion of the wing forward of the torque tube down while the flow continuing over the surface aft of the toque tube is forcing the wing back towards its zero position in both positive and negative deflection cases acting as a restoring force.

5.3   Modifications to wing design based on truck test results

It was clear from the truck testing that the wing needed to be redesigned to address LE deformations. It was decided to use a rigid rib at the center inside the foam and to use the stabilizing force aft of the torque tube to return the LE back to its correct position. The rib was incased in foam after pouring and is only attached to the foam and not the torque tube. It will be referred to as the floating rib. In addition, a carbon fiber stiffener was installed inside the foam near the leading edge. The carbon fiber stiffener had little effect on the torque necessary to warp the wing but provided stiffness to the LE to resist the aerodynamic loading.

The floating rib was made of a composite wood rib cut on the CNC that laid 0.2 in beneath the foam surface and held a carbon fiber LE stiffener in place (Figure 5-9). The rib also had large opens allowing the foam to conform around it. The hole for the torque tube was cut with a large tolerance so that the floating rib can freely rotate. During the pour the rib was CA glued to the carbon fiber torque tube to hold its position, but this glue joint is easily broken once the foam is cured. This new design will be referred to as version 2 (ABv2).
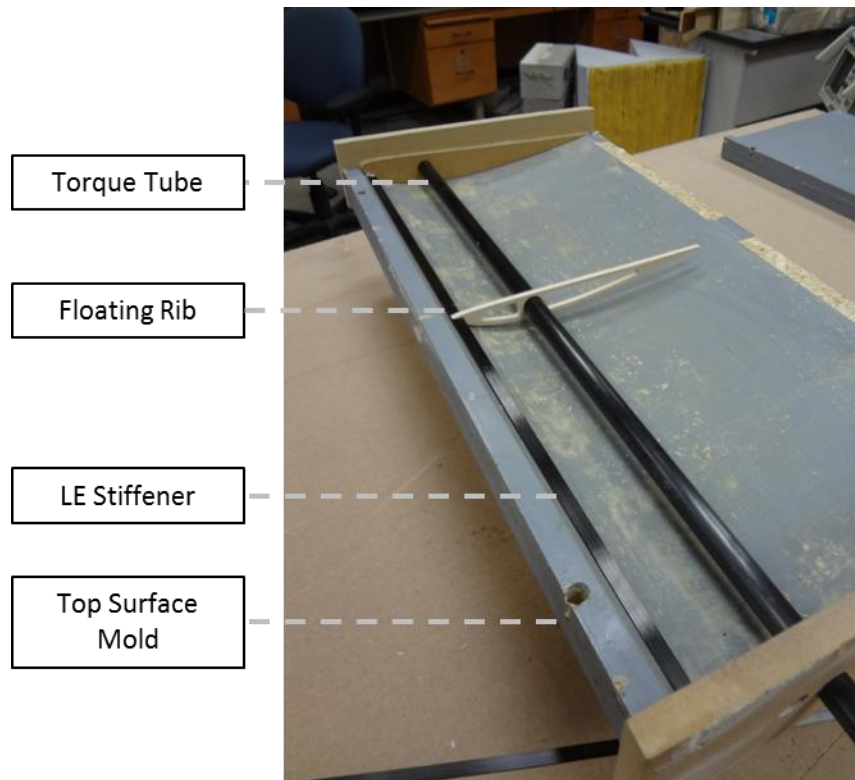
Figure 5-9: Internal supports for Abv2 wings prior to pouring

5.4   Results from ABv2 wing truck test

The same truck tests done for the ABv1 design were also done for the ABv2. Again video was recorded from multiple angles and used examine the wing shape (Figure 5-10).
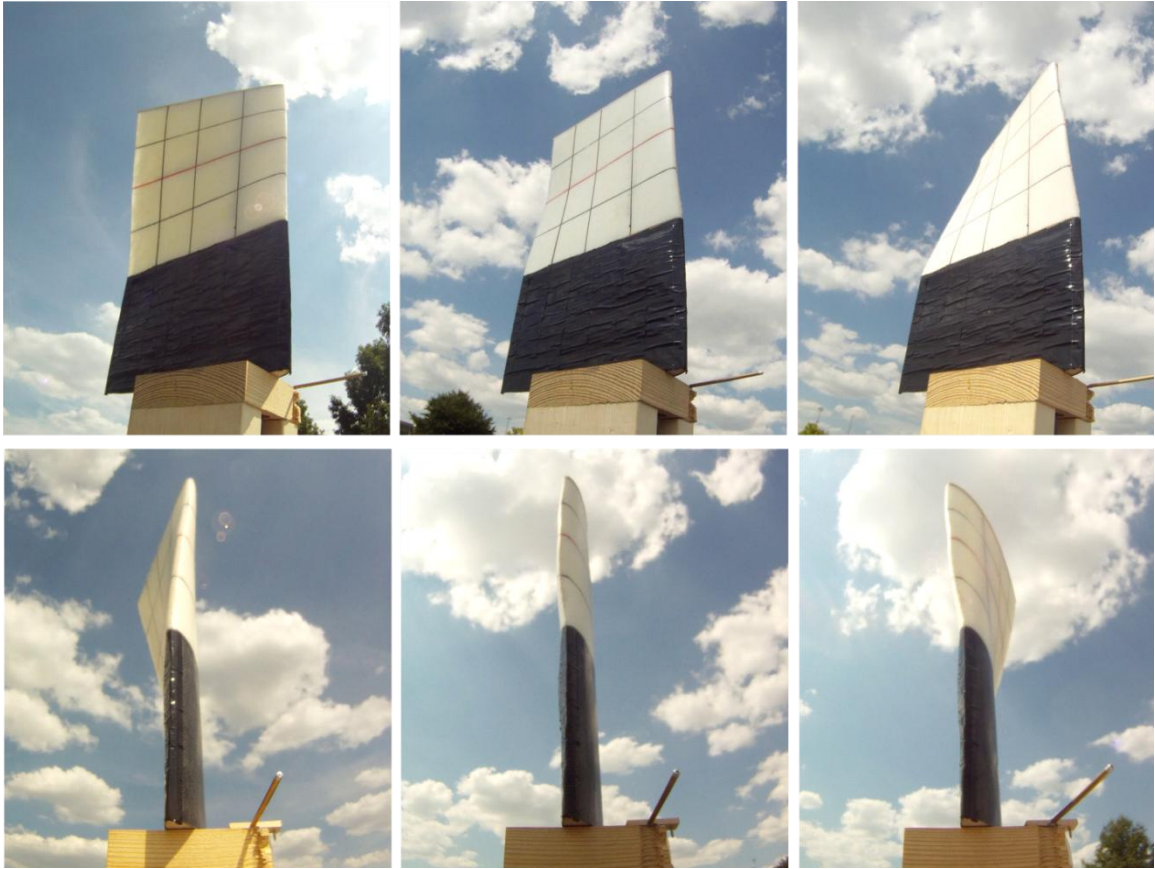
Figure 5-10: ABv2 wing at 40 mph, positive, zero and negative deflection

Between the actuated and floating and between the floating and fixed rib the same behavior can be seen of the LE being deflected downward. But it is less when compared to ABv1 (Figure 5-11).
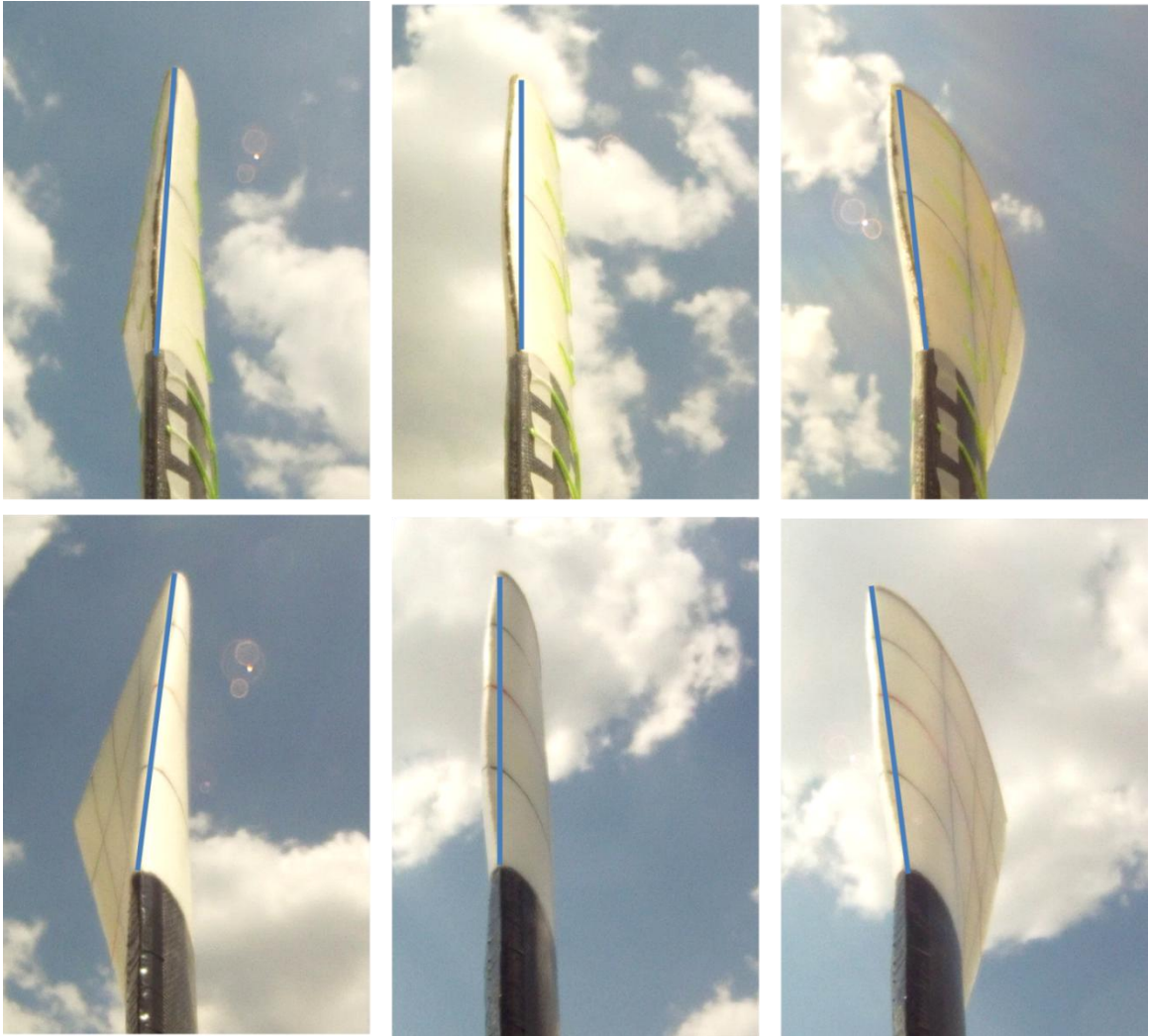
Figure 5-11: Top row ABv1, bottom row ABv2 both at 40mph

5.5   Servo current measurement

Amperage measurements were recorded during each run of the ABv1 wing tests. This was done to confirm that the servo was not being over stressed. The current used by the servo indicates the load on the servo. When the wing is stationary and deflected the servo current increases as the servo turns due to the force of the deflecting foam. But during flight (or truck testing) the servo must also overcome the aerodynamic loads. For a conventional aileron, as the speed is increased or the deflection amount is increased, the load on the actuator increases. From the rough numbers given in the truck test (Table 5-1), it would indicate that in some cases the faster the vehicle moved, the necessary power decreased.

Speed	Deflection		
	Positive	Zero	Negative
0 mph	1.7 Amps	.1 Amps	.9 Amps
25 mph	1.4 Amps	.2 Amps	.7 Amps
40 mph	1.2 Amps	.2 Amps	.8 Amps

This is likely due to a portion of the warping section being forward of the torque tube, acting like a counter balance. Counterbalance control surfaces or control surface horns are often used in small aircraft to decrease the actuation loads an example is in Figure 5-12.

Figure 5-12: Example of a counter balanced control surfaces (www.airmart.com)

As the aircraft continues to increase speed, the aerodynamic forces on the foam acting as a counter balance would increase and eventually become greater than the restoring force of the foam being deformed. The servo would then begin to apply torque in the opposite direction to maintain position. This is potentially why the current increased in the negative deflection case from 25 to 40 mph. Since the current measurement can only be related to the magnitude of the torque and not to the direction, further investigation is not possible without additional sensors. But these results do indicate that wing warping has the potential for decreased actuation forces. While installing strain gauges could lead to a better understanding of the forces, this goes beyond the scope of this thesis.

5.6   Truck testing conclusion

Truck testing proved to be a reliable, safe approach to test the wings and have a better idea of their performance without the risk of flying. While a wind tunnel test would have been ideal, the necessary information was gathered using alternative means.

The truck testing did have its limits. Due to the quick design of the rig, no force measurements were made and would likely have been unreliable due to the turbulent flow over the truck's cab. The AoA was not varied during any of the tests. It would have been beneficial to test at small positive AoA that would have matched those seen in flight. This would have moved the stagnation point from the top surface to the LE or bottom surface causing different loadings on the LE. This consequence of the approach used was not realized until the completion of the test.

Despite that, the TE oscillation that was the initiator of truck testing was found to be a non-issue. The test did allow us to see the larger problem with the LE deformations that, in flight would likely have caused loss of lift and control. The test wing was able to be quickly modified and tested again mitigating the issue and maturing the design to be adequate for flight testing.

6 FLIGHT TESTING

The results from truck testing the second version of the AB foam wing showed that issues with LE deformation had be mitigated and it was safe to start flight testing. While deflection was still seen in the truck tests, it was not oscillatory and not great enough to prevent flight.

The purpose of flight testing was to show that the platform can be flown to evaluate the warping performance of a design. The flight tests also determined if the warping wing can be integrated with a COTS autopilot and if needed special modeling or if other considerations are needed. This was determined through three metrics: pilot feel, aileron effectiveness, and adverse yaw.

Pilot feel is the qualitative analysis given by the pilot as to how the aircraft performs. It is the first to be considered here because it can sometimes be the most telling and does not depend on analysis of telemetry or recovery of an aircraft in the event of a crash. An experienced RC pilot can often quickly diagnose aircraft problems and be able to compensate in the air in a way that many autopilots cannot. The pilot can provide a comparison of performance between aircraft and make decisions concerning normal necessary changes like CG movements and control surface deflections.

Aileron effectiveness is the parameter used to define how quickly the aircraft responds in a roll given deflection of the aileron, or in this case, wing warping. It is the primary value used in the Piccolo autopilot system to design the roll controller. It is important that aileron effectiveness is measured to know how the aircraft will respond, although it is not necessarily an indication of whether the aircraft can be controlled with the autopilot system. A full discussion of aileron effectiveness can be found in Section 2.5. The primary maneuver for analyzing aileron effectiveness is to perform a doublet which starts with the aircraft in steady level flight, and then the ailerons are deflected one direction for a unit of time (typically 1 second) then deflected in the opposite direction. This is typically repeated three times. By comparing the aileron input to the dimensionless roll rate using (2-2) yields the aileron effectiveness.

Pure rolling motion only happens in an ideal aircraft model. When the aileron deflects the aircraft actually responds in yaw and pitch as well. Typically the roll-pitch coupling response is small and can be ignored. Roll-yaw coupling is the result of asymmetric drag in the wing caused by aileron deflection; this effect is often greater and will be examined. Typically roll-yaw

coupling results in adverse yaw, meaning that as the aircraft executes a right roll with the ailerons, the aircraft yaws to the left. To overcome this effect and make a coordinated turn, the rudder is used to overcome the adverse yaw.

All flight tests RC or autonomous were done at the Lexington Model Airplane Club and followed all safety guidelines provided by the Academy of Model Aeronautics (AMA) [42, 43]. In addition, flight tests were performed with a minimum three person crew: pilot, ground station (GS) controller, and ground observer. The pilot controls aircraft throughout the entire flight. During autonomous flight, the pilot monitors the aircraft visually and always has direct control on the flight mode (RC, stabilization, autonomous). The pilot has final say in all decisions concerning the flight. The GS controller monitors the ground station, advising the pilot on aircraft parameters (IAS, altitude, position) when necessary. During autonomous flight, the GS controller monitors the aircraft and can advise the pilot to take control. The third crew member is a ground observer. Their purpose is to observe the entire test flight to make sure all procedures are followed and double checking the aircraft before takeoff. During the flight, they record the flight through video providing a full documentation of the flight and conversation between crew during the flight tests. The ground observer can also assist the pilot with trimming the aircraft and provide information to the pilot or help the GS controller when necessary so that neither has to take their focus off the aircraft.

6.1   Overview of Flight Tests

Following is a summary of each of the five flight tests performed. Each summary includes the aircraft specification, the purpose of the flight test, the flight test plan, and a summary of results.

6.1.1   Flight Test 1 – Control Condition NS Wings (June 13, 2012)

The purpose of this flight test was to confirm the airframe, propulsion, control, and avionics were performing as expected with the conventional wing before switching to the warping wing. The results were also intended to compare aileron effectiveness between the conventional and warping wings.

The standard NS platform presented in Section 3.5 was used with the ArduPlane avionics (Section 3.4.2) (Figure 6-1). The ArduPlane avionics were selected because the same aircraft will be fitted with the warping wing which has increased weight and unknown performance. This

made the ArduPilot ideal because of its low weight and cost. The flight was under RC control with no autonomous or stabilization used. The ArduPlane was only used to collect telemetry.

NS Standard Configuration	
Span	69 in.
Length	56 in.
Chord	10.5 in
GTOW	8 lbs.
W/S	25 oz/ft^2
Dihedral	3°
Airfoil	Modified USA-35B
Avionics	ArduPlane

Figure 6-1: Airframe Specs for – Flight Test 1

The flight plan was to take off, trim the aircraft for steady flight at cruise, and enter a flight pattern parallel to the wind, perform aileron doublets, and finally land (see Figure 6-2 for the flight path).

Figure 6-2: Ground track for Flight Test 1

The aircraft performed as expected and behaved similarly to other NS platform aircraft. A total of four aileron doublets were performed. The aircraft landed with no issues.

Using the ArduPilot telemetry the aileron position, roll angle, gyro and IAS data were examined for each doublet case. Servo position was recorded by the ArduPilot as a pulse-width modulation (PWM) signal which varies the length of a square wave signal to define a position. The length of this square wave in microseconds was recorded. The industry standard for these servos is a 1500μs pulse for the neutral position and 10μs/° rotation. Due to the linkages of the aileron, the rotation of the servo and the aileron are not one to one. Calibration for conversion from the PWM number to the aileron position was performed prior to the flight. Two servos are used for aileron control, one for each semi-span. The ailerons are installed with aileron differential to mitigate adverse yaw effects. The two positions are averaged for the calculation of aileron effectiveness. The servo position was recorded at 17Hz.

Roll angle was calculated by the ArduPlane and is a function of gyro, accelerometer, and magnetometer sensor data. This roll angle was sampled at a rate of 17Hz. Roll rate data is acquired from the 3-axis gyro and recorded at 50Hz. The sign convention for all angles and angular rates is shown in Figure 6-3. IAS was determined from the pitot-static pressure transducer and was recorded at 17Hz.
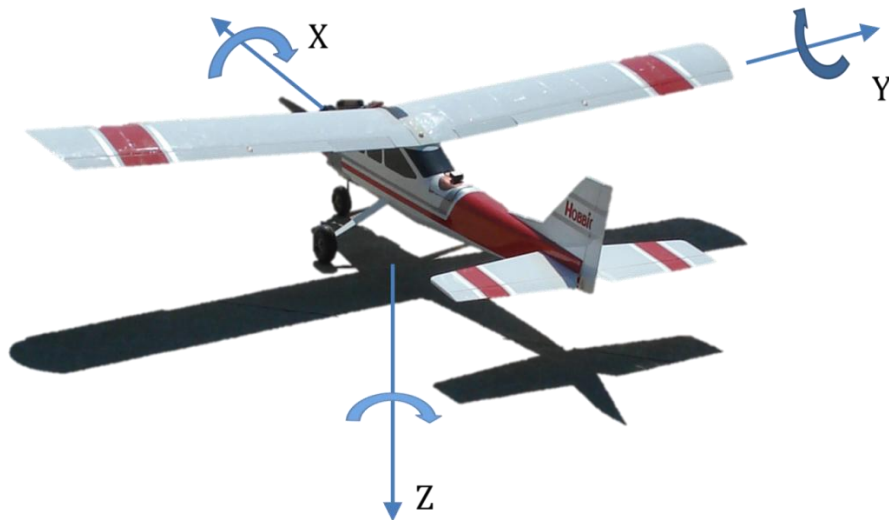
Figure 6-3: Coordinate system orientation for sensors
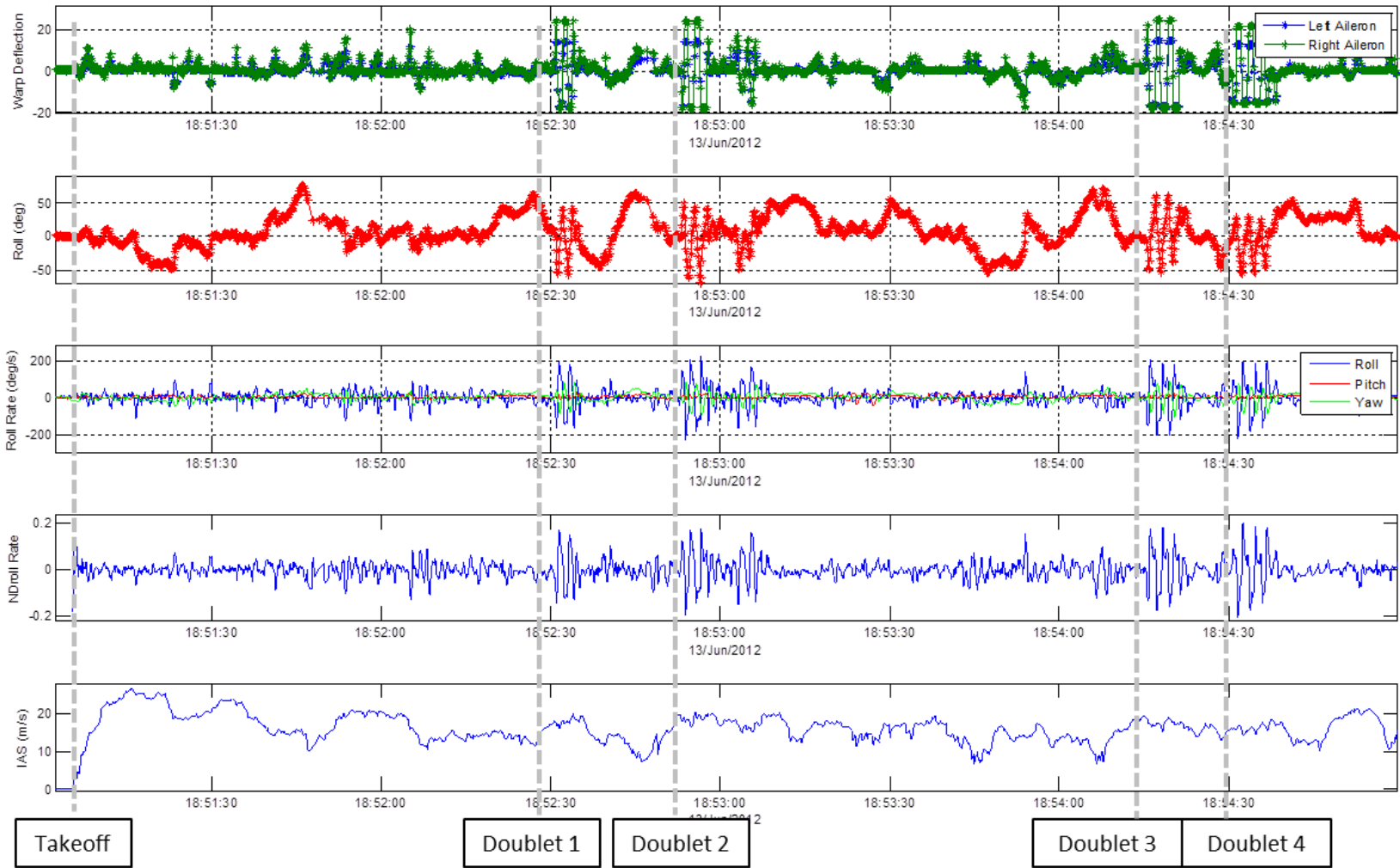
Figure 6-4: Time history for Flight Test 1

The complete time history of aileron deflection, roll, roll rate, non-dimensional roll rate, and IAS for the flight can be seen in Figure 6-4. Dimensionless roll rate was calculated from the telemetry using (2-1). The figure has markers for takeoff, the begging of each doublet set and landing.

Figure 6-5 shows the aileron deflection and dimensionless roll rate for Doublet 3. The time history shows that while the input of aileron deflection was a square wave the response of the roll rate was not, showing a potential second order response. This was later identified to be the result of using too large of deflections resulting in the aircraft rolling quickly to roll angles of +/-45° or more. This meant that by the guidelines for determining aileron effectiveness discussed in Section 2.5 this data was not valid. However, this did show that the ArduPilot telemetry would be sufficient in characterizing the warping wings. It was decided to not re-fly this flight for doublet data since similarly configured NS platforms have been flown extensively at UK and aileron effectiveness determined through doublets.
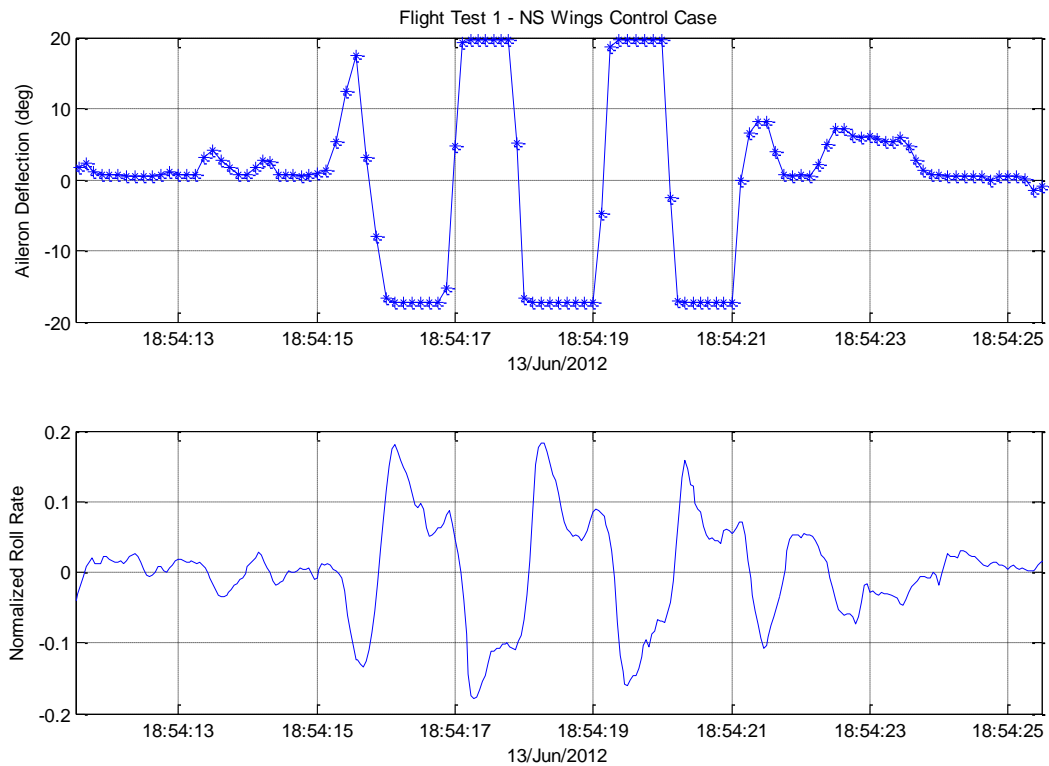
Figure 6-5: Aileron deflection and dimensionless roll rate during Doublet 3

The aircraft performed nominally concerning roll yaw coupling compared to the pilots experience with other NS platform aircraft. Figure 6-6 shows the aircraft's response through an

68

aileron doublet maneuver. The first plot shows the aileron input, the second the attitude angles, and the third plot shows the attitude rates. As expected, as the aircraft rolls through the doublet the pitch gyro remains near zero, indicating that there is no coupling between the roll maneuver and pitch. However, as the aircraft rolled the yaw gyro showed that the aircraft yawed in the opposite direction. During the doublet the rudder and elevator remained fixed meaning the motion is the result of the ailerons. The aircraft was experiencing adverse yaw. For the same reason that aileron effectiveness was unable to be calculated, the adverse yaw could not be quantitatively analyzed.
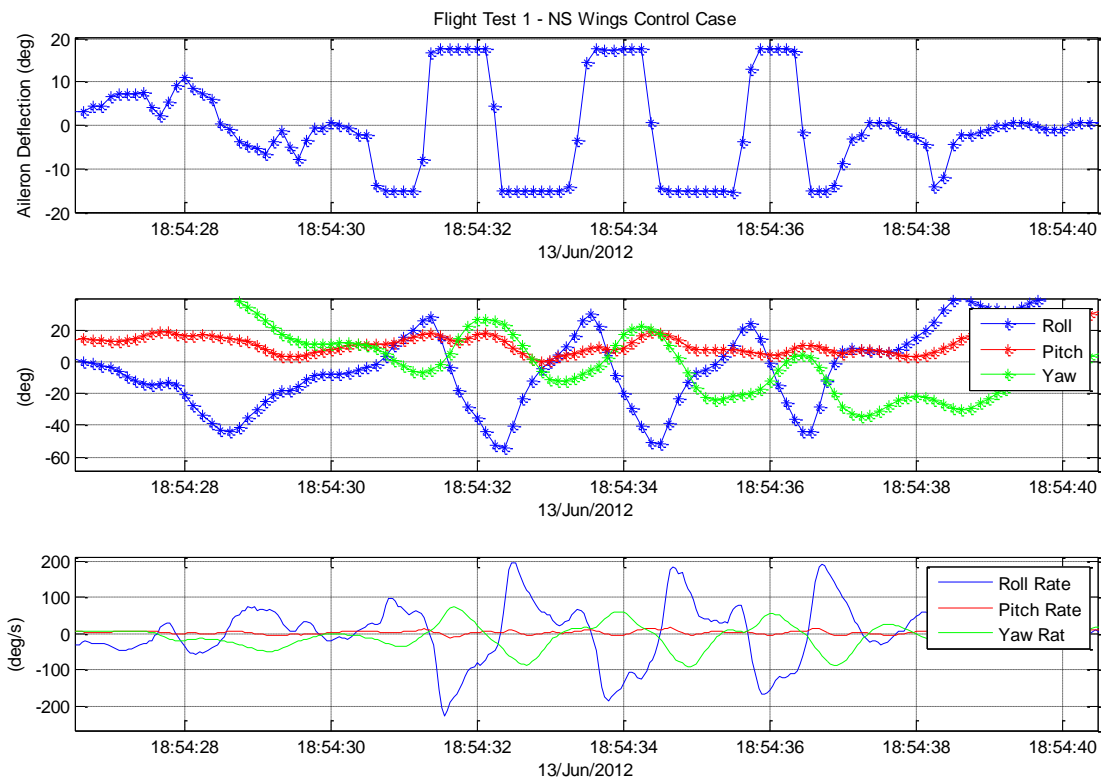
Figure 6-6: Plots to examine roll-yaw coupling

The first flight test was successful in that data was collected and any issues concerning the aircraft systems separate from the warping were addressed. This also served as a practice run for the ground crew establishing responsibilities and procedures. The data collected was not able to be quantitatively characterized due to the doublets causing the aircraft to roll well outside the linear response region. However, the pilot was able to provide qualitative information about the flight. The flight was not re-flown out of interest in moving forward and that previous data for similarly configured aircraft existed.

6.1.2 Flight Test 2 – First Wing Warping Flight (June 16, 2012)

The purpose of the second flight was to prove the operation of the warping wings. The same aircraft used in the previous flight test was used except the standard NS wing is replaced with the warping wing detailed in Chapter 4 as well as using the final version of the AB foam inserts described in Section 4.5 (Figure 6-7). The pilot console was setup with a three position switch allowing the pilot to switch between the backup conventional ailerons, warping, or both for roll control. The pilot console was also setup to allow the conventional ailerons to be used as flaps.

Warping Wing Configuration	
Span	73 in.
Length	56 in.
Chord	10.5 in
GTOW	10.5 lbs.
W/S	31.6 oz/ft^2
Dihedral	0°
Airfoil	USA-35B
Avionics	ArduPlane

Figure 6-7: Airframe Specs for maiden flight of warping wings – Flight Test 2

The flight plan was to take off using ailerons only until a safe altitude was reached. Then trim the aircraft while in a flight pattern paralleling the wind. Then control would be switched from the conventional ailerons to warping. The pilot would then begin with small control inputs to determine the response characteristics. Once the aircraft responded in a stable and predictable way, the pilot could move on to performing doublets. The test protocol was that if at any point in the flight the aircraft showed signs of instability due to warping actuation the control will be switched back to the ailerons. Depending on the severity of the instability, the aircraft will either be landed or climb to attempt the maneuvers again.

The day of the flight tests, the winds were 10-15 mph along the runway. From a series of high speed taxies, it was decided to use flaps for the takeoff. Only the ailerons were used for roll control during the takeoff and climb out. The aircraft rolled down the runway and lifted off with a steady climb rate and performed similarly to the regular NS platform. The flight path was parallel to the run way and the wind with a typical box pattern. During some longer straight runs

of the flight it was necessary to turn opposite to keep the aircraft over the LMAC property forming a figure eight (Figure 6-8). This also meant that the aircraft was tested in a left and right hand pattern. The ailerons were noted by the pilot to have minimal authority, requiring large inputs, but the aircraft was controllable. The aircraft only required minimal trimming. After it entered steady level flight, two warping doublets, one aileron doublet, and one doublet with both aileron and warping were performed. The aircraft performed perfectly and predictably throughout the entire flight. The pilot observed that the aileron-only authority was minimal, requiring large inputs to control the aircraft. The warping provided significantly greater control authority requiring typical input magnitudes. When both aileron and warping were used the aircraft was very quick to roll, but still stable. The flaps remained lowered throughout the flight to decrease cruise velocity and therefore providing a greater margin in the relatively high winds. The wing warping performed similarly to conventional aileron control and the pilot had no issues transitioning between the different roll control mechanisms. Due to the low aileron effectiveness of the aileron-only configuration, the landing was performed under wing warping actuation only.
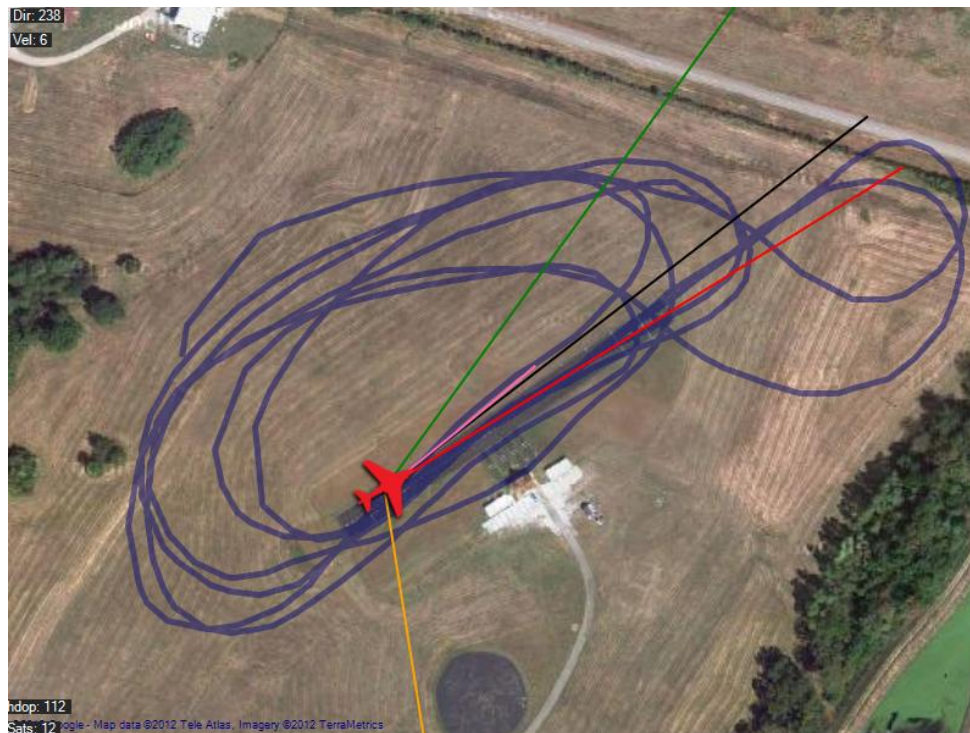
Figure 6-8: Ground track from Test Flight 2

71

Figure 6-9 shows the complete time history of the flight with the doublets marked. Figures 6-10-12 shows the plots for each of the three doublet conditions. These doublets like the first flight were controlled by the pilot but this time the pilots' input is closer to a ramp input than a step input. This was likely due to this being the first flight and the pilot not feeling comfortable committing to the doublets, which requires a predefined set of stick deflections regardless of the planes behavior. This can be difficult for the pilot to commit to on an untested aircraft's maiden flight. In addition, the doublets attempted, much like the first test flight, had too much deflection causing the plane to roll past 45°.
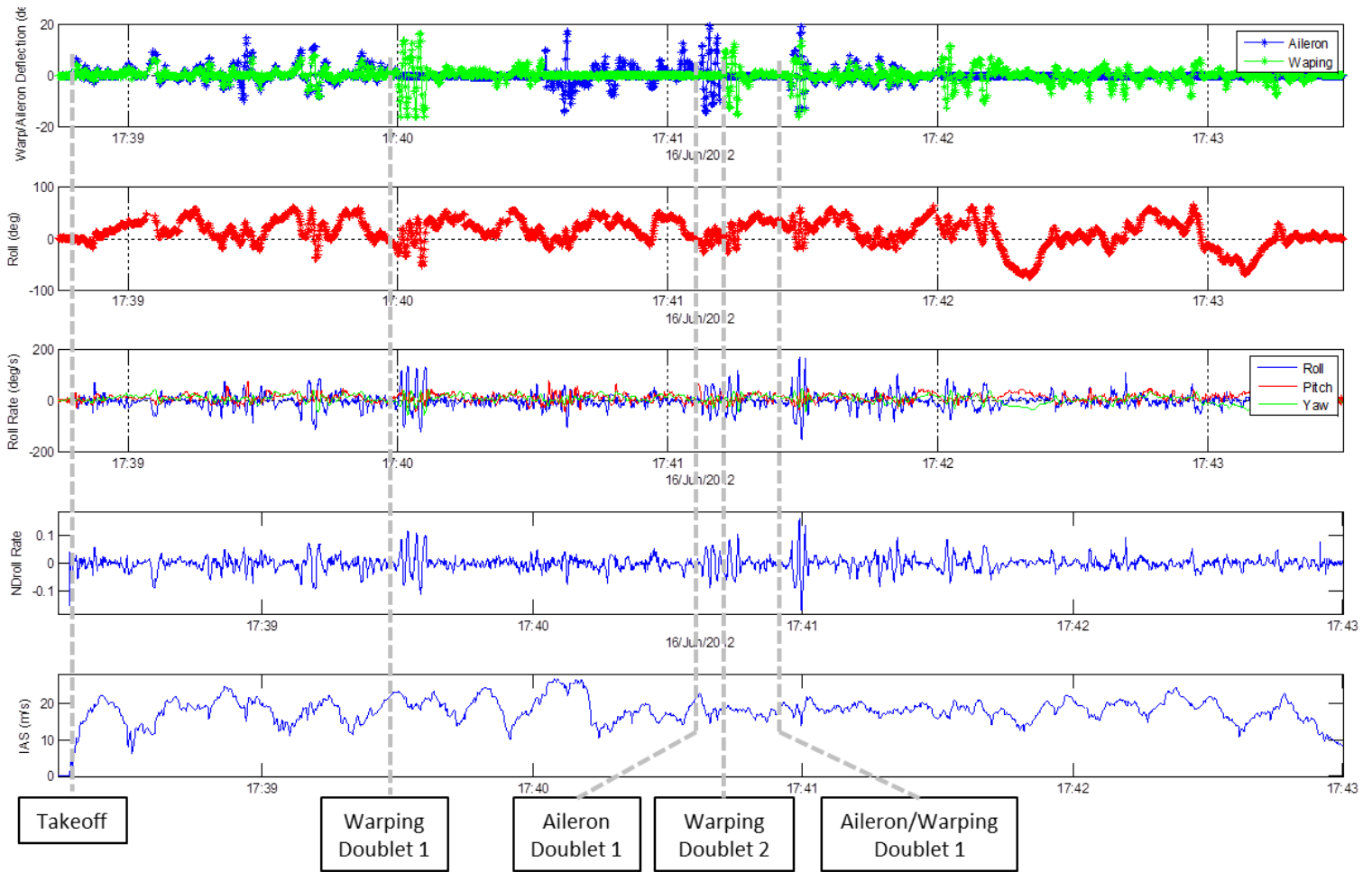
Figure 6-9: Time history for Flight Test 2
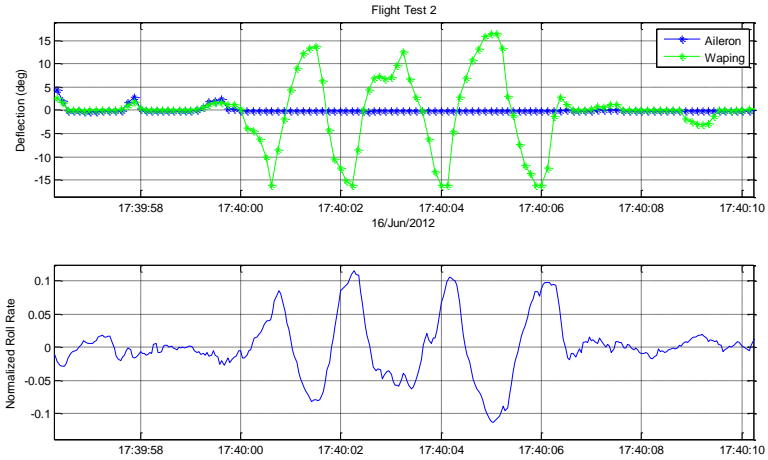
Figure 6-10: Doublet for warping actuation
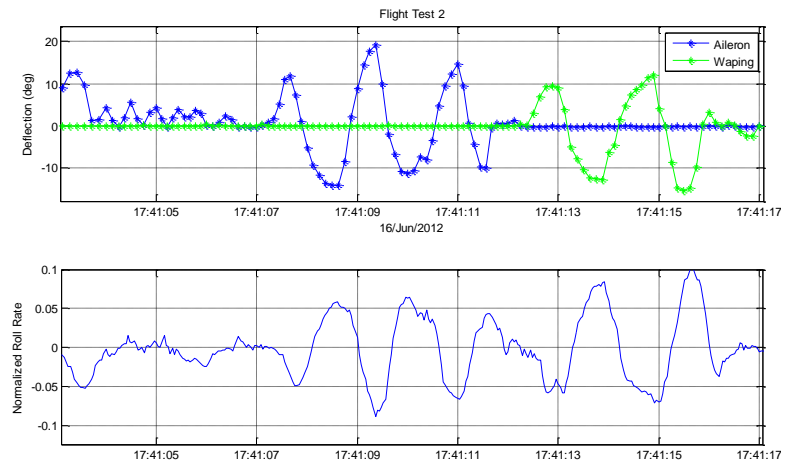
Figure 6-11: Doublet for aileron actuation
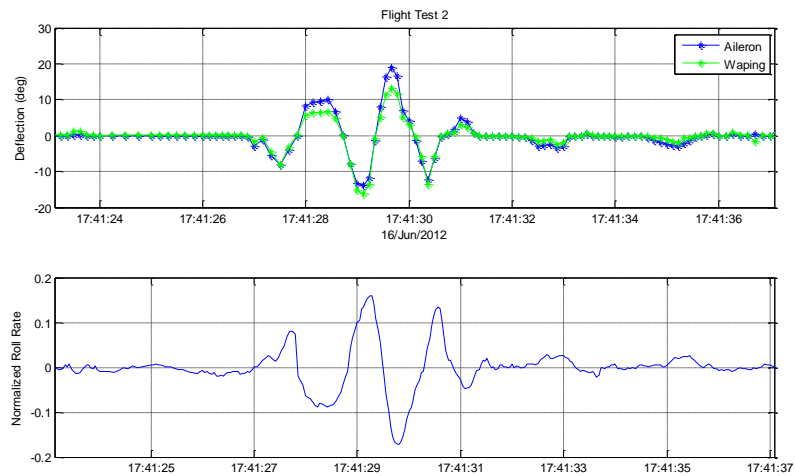
Figure 6-12: Doublet for both actuation of aileron and warping

74

In addition, to ArduPilot telemetry the aircraft was equipped with cameras to view the warping section during flight. Two video cameras were used in fixed positions on the aircraft, along with one camera on the ground.

A HD GoPro camera was mounted in place of the rear hatch looking forward at the TE (Figure 6-13). A low definition bullet camera was mounted in the forward hatch looking aft at the LE (Figure 6-13). The cameras are mounted so that the field of view (FOV) covers the maximum amount of the warping section possible (Figure 6-14). Only the port section was observed during testing. Both cameras record to onboard SD cards. Wireless transmitters were not used due to the additional weight and limited value of monitoring the wing during the flight. The SD cards used in the cameras have been proven to survive crashes during other projects in the UAV lab at UK, so the risk of losing data was minimal.
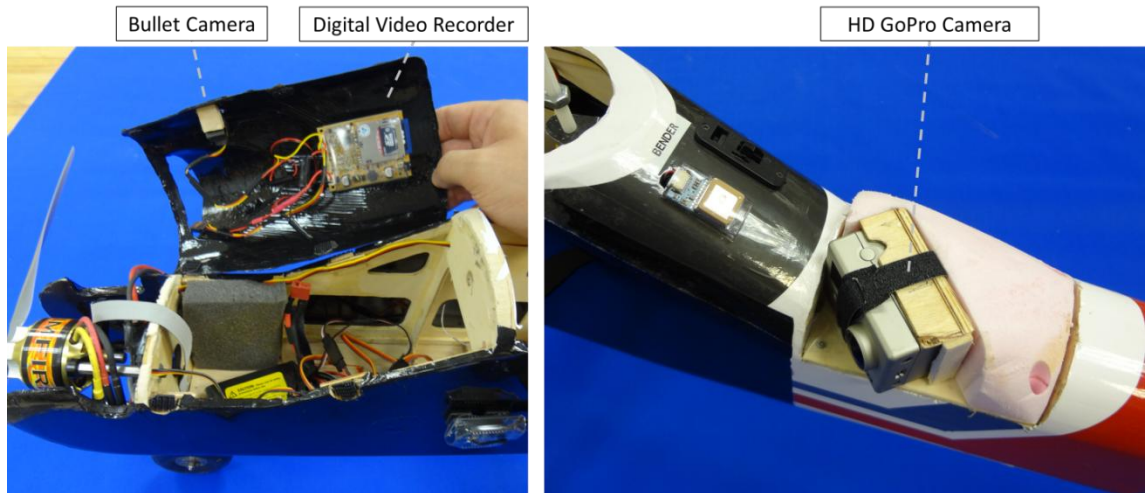
Figure 6-13: Cameras mounted on aircraft
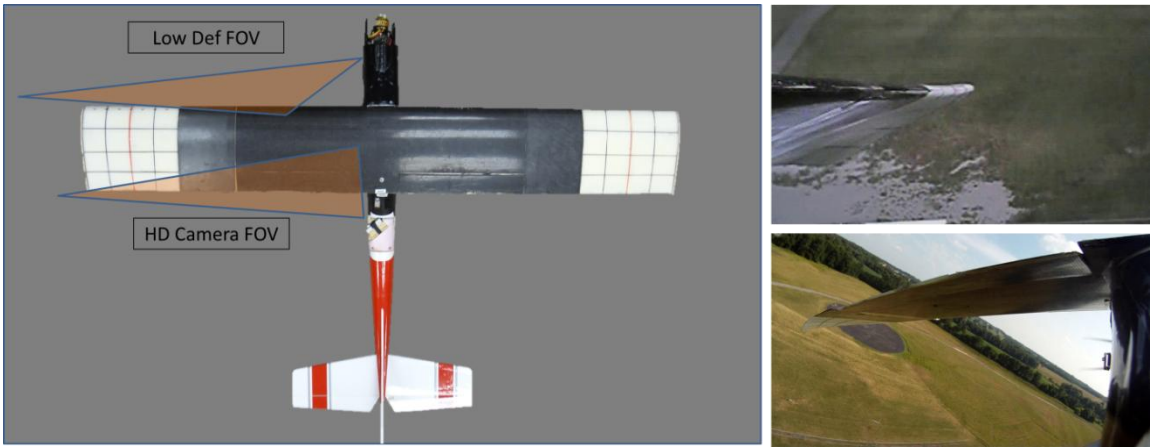
Figure 6-14: Camera positions and field of view (FOV)

Figure 6-15 shows the full frame views from the cameras during steady level flight. In order to show the warping section more clearly in following figures the camera view will be cropped.

Figure 6-15: Full frame views from cameras during steady level flight at cruise

During cruise at 15-20kts the wing held its shape better than expected from the truck testing (Figure 6-15). This is most likely because the wing is operating at a positive AoA in flight verses the zero AoA during truck testing. In the doublet maneuvers, the wing can be seen being deflected and holding its actuated shape but there is still some drop in the LE and some upward deflection of the TE at the center of the warping section (Figure 6-16, Figure 6-17).

Figure 6-16: Wing shape during left roll of doublet

Figure 6-17: Wing shape during right roll of doublet

During the flight the g-loading was kept minimal; the greatest loading was during a small pull-up maneuver which was also the highest speed reached during the flight of 26kts and 1.5g. During this maneuver, the wing can be seen deflecting the most of all flight conditions (Figure 6-18). Despite the deflection, both wingtips maintained lift and no roll input was necessary to keep the wings level during the pull up.

Figure 6-18: Wing shape during 1.5g pull-up at 26kts

6.1.3   Flight Test 3 – Attempted Transition to Stabilized Flight (July 17, 2012)

The purpose of this test flight was to transition to stabilized flight as a first step to autonomous flight control. The aircraft had previously been operating in manual mode, where the pilots stick and other commands are directly converted to control surface commands and sent to the aircraft (Figure 6-19). As an example, the pilot's right sticks vertical position is converted to an elevator angle in the pilot console, that signal is sent to the receiver, and then

to the ArduPilot where is it logged and sent directly to the servos. The pilot's right horizontal stick position actually controls multiple servos. The Roll/Flap Mix Program seen in Figure 6-19 takes in the inputs of: stick position, the roll control mode (warping, aileron, or both) and the desired position of the flaperons; and outputs signals for the: port warping, starboard warping, port flaperon and starboard flaperon servos. This mixing was done in the pilot console on the ground and the four individual signals sent via 2.4Ghz to the receiver and ArduPilot.
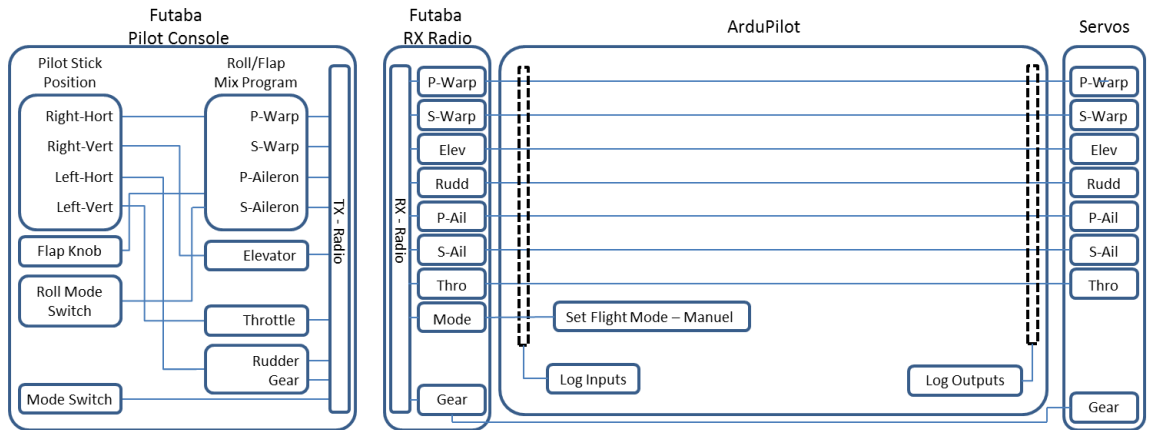
Figure 6-19: Signal schematic for manual mode

In the stabilization mode known as Fly-By-Wire_A (FBW_A) in the pilot's console, configuration remains the same but when the switch marked mode in Figure 6-20 is moved from the manual to FBW_A position the ArduPilot changes programs. In FBW_A mode, the ArduPilot converts the signals typically used for port-warp servo position and elevator servo position and converts them to desired roll and pitch angle respectively. It then used those values in a control system to send signals to the warping, elevator, and rudder servos (Figure 6-21). This meant that in FBW_A mode the pilot's stick which typically controlled the ailerons and elevator directly now controlled the roll angle and pitch angle.
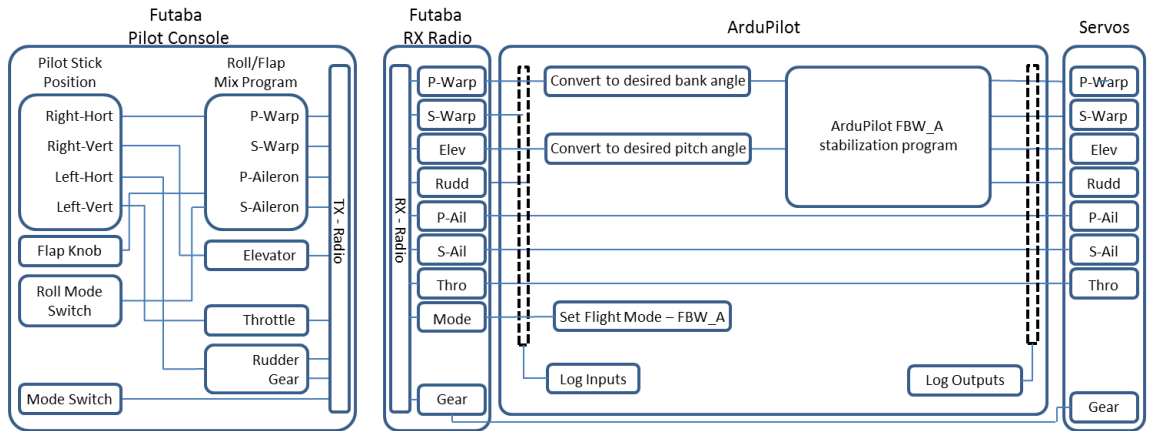
In FBW_A mode the ArduPilot did not have control of the flaperons or throttle which were left to the pilot to control. In a more advanced stabilization program (FBW_B) the ArduPilot can control these signals and implements an altitude, velocity, and heading hold. Due to the ArduPilot only having eight channels the nose gear steering signal was sent directly from the Futaba radio to the servo. This was not an issue since the aircraft was always landed in manual mode and the nose gear position was not of importance for telemetry.

For both manual and FBW_A the ArduPilot recorded the input and output signals for each channel. During manual mode the input and output telemetry will be identical.

The flight plan was to use the same aircraft configuration outlined in Flight Test 2; the plane would take off in manual mode, establish a flight pattern at a safe altitude, and during the straight leg of the pattern the pilot would switch to the FBW_A mode. If the plane continued straight and level the pilot would continue to fly the pattern in FBW_A mode. If the plane deviated from straight and level after switching to FBW_A the plane would be returned to manual mode. Depending on the nature and severity of the deviation from straight level flight the aircraft would either climb higher and attempt the transition again, or the test would move on to the secondary objective of aileron doublets.

As with the first two flights the aircraft took off under manual mode and climbed to altitude without incidence. Once the plane was trimmed the first attempt at transition was made. Immediately after the switch the plane nosed over quickly eventually reaching a -20° pitch angle before it was decided the autopilot was not going to recover and the pilot took

control returning the aircraft to level flight. During this approximately one second period the aircraft remained level in roll and only responded in pitch. This was attempted again later in the flight with the same result. Figure 6-21 shows the aircraft response in pitch (blue), the elevator angle (red) and the pilot's elevator stick position (green) during the transition and recovery. The figure shows that the at the transition point the ArduPilot immediately set the elevator to -5° causing the aircraft to pitch down. At the same time it shows the pilot's stick position remaining nearly fixed at the trim point, which should command the ArduPilot to maintain a fixed attitude. The ArduPilot slowly increases the elevator as the aircraft pitched down.
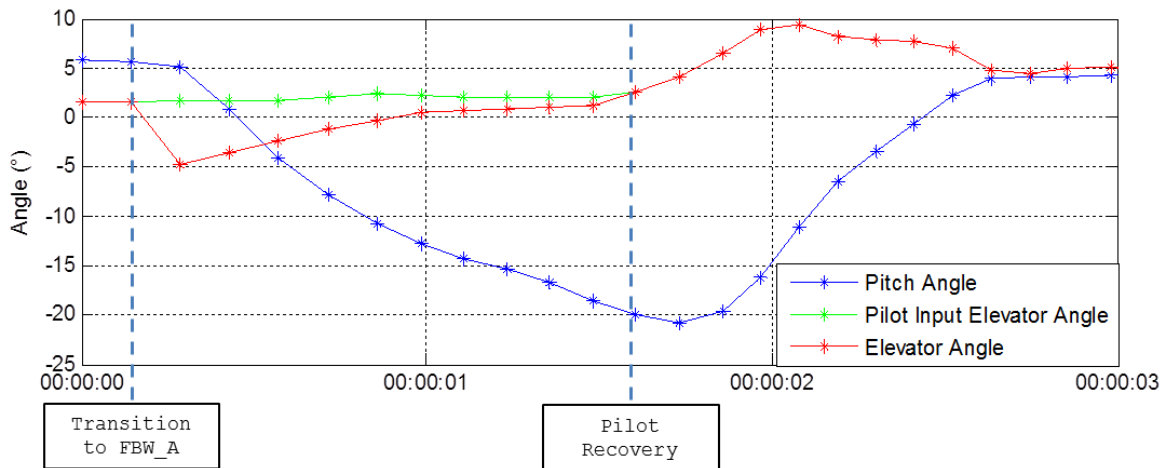
Figure 6-21: Aircraft response during FBW_A transition

The aircraft was landed with no issues. To identify the problem on the ground the aircraft was powered on but without propulsion and put in FBW_A mode. Then by hand, the aircraft was pitched up and the elevator could be seen deflecting down to counter the pitch up. The same was seen for the pitch down. Next with the aircraft on a bench top, the flight mode was changed between manual and FBW_A, each time the elevator immediately deflected down. It was confirmed by the ground crew that the plane did not do this during similar preflight checks. After looking through the flights telemetry it was identified that during the climb out the aircraft was trimmed in the pitch direction by the pilot on the pilot console. However, the ArduPilot's trim points were calibrated with the pilot console during preflight which meant that once the pilot changed the trim point the signal being sent had an offset in the PWM number when compared to the ArduPilot's calibrated trim point. In FBW_A mode this difference would be interpreted by the ArduPilot as a command to establish a non-zero pitch angle proportional to

80

the difference between the new trim point in the pilot console and the trim point set in the ArduPilot during preflight.

The fix for this issue was to have the aircraft trimmed for flight before calibrating the servo positions. Unfortunately, this meant that the pilot could not trim the aircraft during flight before transitioning to FBW_A. However, since this aircraft had already flown several times and the configuration was not changed the trim points remain fairly close, meaning it is only a minor inconvenience for the pilot and should not affect the flight otherwise. In the future the pilot console can be setup with multiple trim schemes which with automatically change when the switch controlling the flight mode is changed.

6.1.4   Flight Test 4 – Second Attempt at Transition to Stabilized Flight (July 21, 2012)

With the pitch issue in FBW_A mode found in Flight Test 3 resolved the plan for the fourth test flight was identical. The only difference being that the pilot would not trim the aircraft during flight. If trimming was absolutely necessary the aircraft would be trimmed then landed, and the ArduPilot's trims reset and the flight would then continue from there.

Again the aircraft took off with no issues and established a rectangular flight pattern at altitude before the transition was attempted. With the first transition the aircraft maintained its attitude and continued straight and level for approximately ten seconds before being returned to manual mode at the end of the straight leg of the pattern. On the second attempt the pilot attempted to use the sticks to "steer" the aircraft in FBW_A mode with small inputs which in FBW_A should command a roll angle. The aircraft was not seen visually responding. On third attempt in FBW_A maximum stick deflections were used which should have commanded the aircraft to bank to the set maximum bank angle of. The aircraft was observed banking but at an angle much smaller than 30° and yawing in the opposite direction of the bank. From the ground it was unclear why the aircraft was not responding so flight mode was changed to manual and the aircraft landing.

Viewing the telemetry showed that the aircraft did roll in the direction of the commanded roll, but the aircraft was unable to achieve the 30° roll angle. The telemetry for the control surface positions showed that the warping servos deflected in the correct direction which can be seen Figure 6-22 with a positive deflection causing a positive/right roll but the ailerons

deflected in the opposite direction. This was confirmed by the aft onboard camera (Figure 6-23 Figure 6-24).
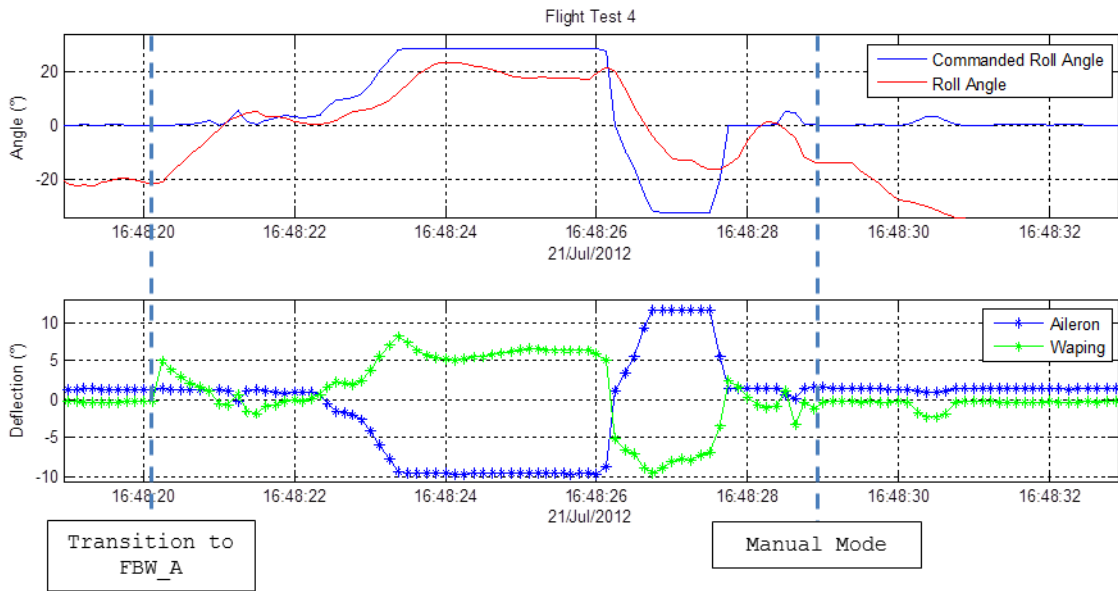
Figure 6-22: Aircraft response and control surface position during FBW_A

Figure 6-23: Control surfaces during right roll, note aileron deflected for left roll

Figure 6-24: Control surfaces during left roll, note aileron deflected for right roll

It was determined during post flight ground testing that the pilot had left the roll mode switch in the position which causes both aileron and warping to be used. The ArduPilot in FBW_A mode interpreted the warping signals as commanded roll rates and attempted to roll the aircraft. However, the ArduPilot did not have control of the ailerons (Figure 6-20) and due to a sign error in the ArduPilot the ailerons deflected in the opposite direction. Despite that the aileron acted opposite the commanded roll direction the ArduPilot was able to use the warping actuation to roll the aircraft but not to the desired roll angle.

This meant that on the next flight before transition the pilot would have to set the roll mode switch to warping only. This way there would be no signal sent to deflect the ailerons during the FBW_A flight.

6.1.5   Flight Test 5 – Successful Stabilized Flight (July 21, 2012)

The plan for the fifth test flight was the same as the previous two flights. The previous issues were addressed and specific procedures for the pilot during the test were set. The aircraft remained in the same physical configuration.

Again the aircraft took off and established a pattern, once at altitude three separate transitions to stabilized flight were attempted and more aileron doublets were performed at the end of the flight.

Figure 6-25 shows the ground track of the entire flight with the red markers showing the portion of the flight in FBW_A mode. With each transition the aircraft continued straight and level and with each one the pilot used the roll control stick to "steer" the aircraft increasing

83

amounts. The third stabilization run was the longest and is highlighted on the right in Figure 6-25. This portion of the flight will be examined in detail below.
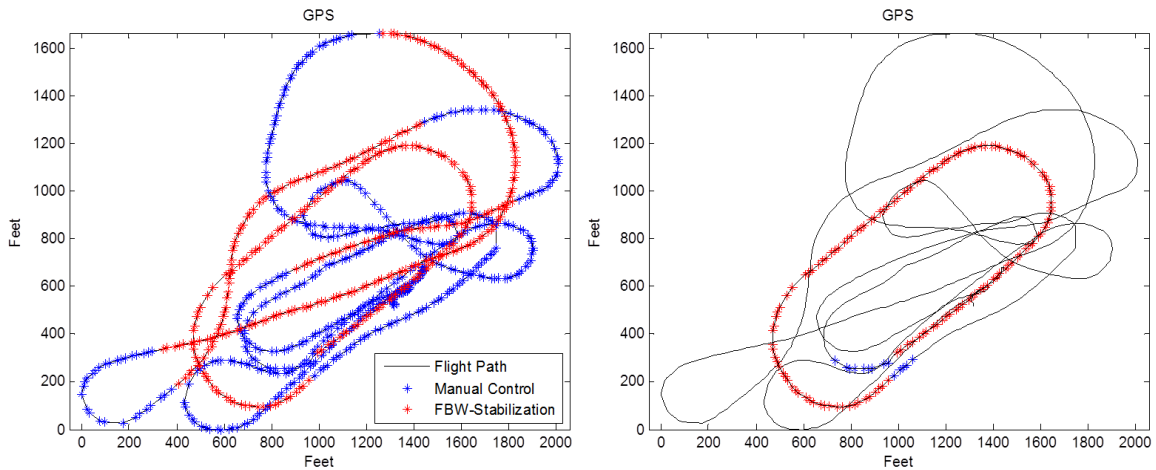
Figure 6-25: Left) GPS ground track of fifth flight Right) Portion of the flight to be examined further

The top graph in Figure 6-26 shows the aircraft response in roll angle (red) compared to the input of commanded roll angle (blue) which is decided by the pilots stick position which is typically used for aileron control in manual flight. At the beginning of the time history when the aircraft is proceeding straight and level, at just after 17:26 the aircraft begins a left roll resulting in a 180° turn. It then goes back to straight level flight before starting another left hand turn.

It's clear from Figure 6-25 and Figure 6-26 that the aircraft is capable of following the commands from the pilot for turning. Though Figure 6-26 shows that the ArduPilot control gains still need to be adjusted as there is a noticeable oscillation of the aircraft in roll in the straight portions of the flight.
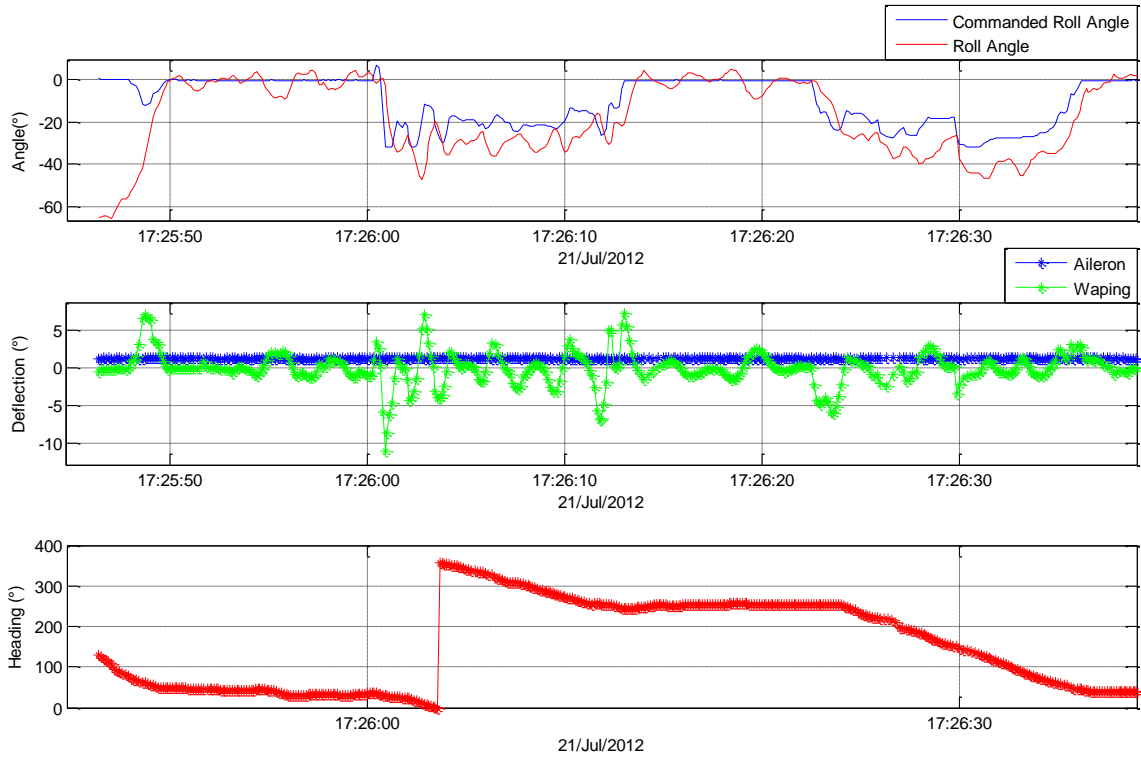
Figure 6-26: Telemetry during FBW_A stabilization

During some of the manual control portions of the flight aileron doublets were performed. Due to the lessons learned in precvious flights the doublets were correctly performed resulting in ten doublets. Figure 6-27 shows a portion of the telemetry used to calculate the values obtained in Table 6-1. An average value over the ten doublets of 0.32 was determined for the aileron effectiveness. This value corresponds closely by the value predicted through AVL models of 0.33 [44].
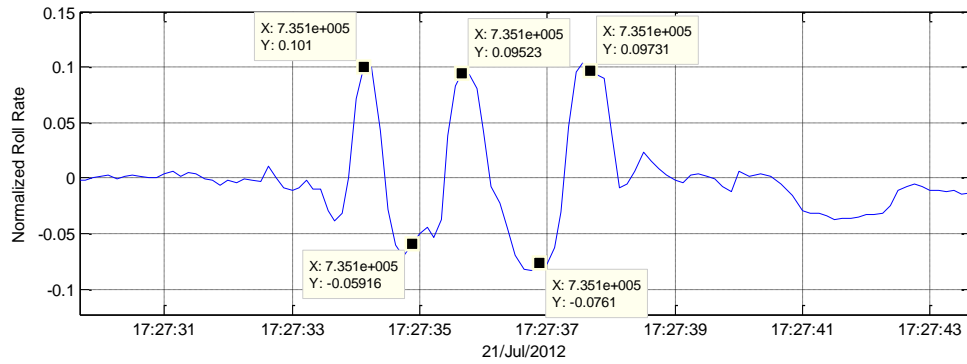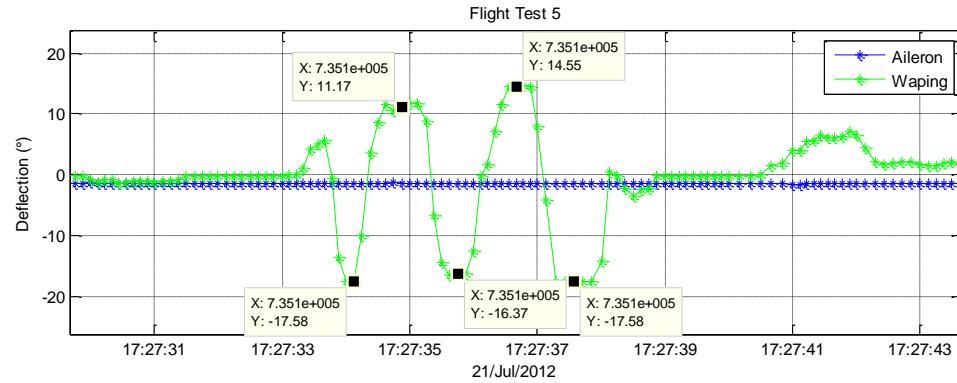
Figure 6-27: Aileron doublet telemetry from Flight Test 5

Table 6-1: Aileron effectiveness from Flight Test 5 doublets

Doublet	δ_1	δ_2	$\bar{p}_1$	$\bar{p}_2$	Al Eff
1	-0.09°	-17.54°	0.0045	0.1062	0.3341
2	-17.54°	14.68°	0.1062	-0.0798	0.3309
3	14.68°	-17.54°	-0.0798	0.0983	0.3168
4	0.35°	-17.58°	-0.0016	0.0997	0.3240
5	-17.58°	14.68°	0.0997	-0.0786	0.3169
6	14.68°	-0.61°	-0.0786	0.0056	0.3157
7	-17.58°	11.17°	0.1002	-0.0592	0.3177
8	11.17°	-16.37°	-0.0592	0.0952	0.3214
9	-16.37°	14.55°	0.0952	-0.0761	0.3176
10	14.55°	-17.58°	-0.0761	0.0973	0.3094

6.2   Flight Testing Summary

The purpose of the series of flight tests described above was to show that this platform with unique warping wings could be flown and the dynamics measured through onboard

telemetry. Using the telemetry several issues were addressed for both the development of the platform and for the integration of warping with a COTS autopilot system.

Ultimately the aircraft was able to be controlled through stabilization from the autopilot system. Despite that fully autonomous flight was never shown with the ArduPilot the next step would be a waypoint following navigation routine. The ArduPilot is based on a cascade PID control system with the outer control system being the navigation which sends desired roll and pitch angles to the inner control system. By demonstrating flight in the FBW_A mode it eliminated the outer navigation control loop, and the pilot acted as the outer navigation loop sending roll and pitch angle commands directly to the inner control loop. Though more tuning could be done, the roll/pitch control system is ready for the addition of the navigation controller. This final step was not completed due to time restraints. But the same wing was flown autonomously with a Piccolo II Autopilot system with a similar cascade PID control system after the defense of this thesis [44].

7 CONCLUSION

7.1 Summary

The goal of this thesis was to design a warping wing for the purpose of testing warping methods to be used with inflatable wings for autonomous flight control. The work covered in this thesis addressed several of the challenges for solving wing warping for autonomous flight control. A unique rapid prototyping method was developed, a means of quickly ground testing design was used and finally the wing was flight tested to measure its characteristics in flight.

Due to the many challenges of working directly with inflatable an alternative way of prototyping the warping designs was developed. The use of deformable foams allowed for designs to be quickly and cheaply developed. The use of AB foam allows rigid structures to be imbedded in the wing along with alternative warping mechanisms. This allows the warping sections to be tailored to match desired stiff ness. Now that the method has been developed several designs can be fabricated and ground tested in a single week at a fraction of the cost of single inflatable wing.

As an alternative to wind tunnels a truck was used to test warping wing sections on the ground prior to flight testing. These tests were able to identify several issues with the initial design and allowed for quick testing of subsequent designs.

With successful ground testing the warping design needed to be flight tested to show that it would be controllable with a COTS autopilot system. Each flight test was meant to be incremental building on the previous tests and isolating and testing various components as independently but also efficiently as possible. The first flight of the warping wing showed that the aircraft could fly and onboard video showed that the wing behaved similarly to how it had during truck testing. Subsequent flights worked towards the goal of autonomous flight. The aircraft was very easy to fly and control. The pilot found the warping response to be very similar to ailerons and elected to perform all landings using warping instead of the ailerons due to their stability and control. Ultimately, the warping wings were flown for 18 minutes, with an average cruise speed of 38kts and reaching a maximum speed of 60kts. The aircraft during brief pullouts exceeded 2g of acceleration with no damage to the wing or instability during the pullouts. Using warping a max roll rate of 145°/s was achieved during a doublet maneuver and the aircraft was routinely banked 50° degrees for turning in manual operation even reaching a max bank angle of

100°. The aircraft never showed signs of instability and had five perfect landings requiring no non-routine maintenance. In the experience of this author for flight testing aircraft of this nature this is an exceptional record most likely attributed to the strict series of check lists and preflight procedures developed in the UK UAV lab over the past two years. The aircraft made several successful transitions between manual and stabilized flight. During stabilized flight the ArduPilot was able to maintain steady level flight and follow the bank angle commanded by the pilot. After the defense of this thesis the same wing was flown under completely autonomous control using a Piccolo II Autopilot system.

7.2   Future Work

Future work should start by iterating on the current design. The design was built very conservatively since it was a first and has room for optimization. Looking at ways to increase material stiffness should allow for longer warping sections to be used. This could really show the potential of wing warping since smaller deflection would be needed. This could ultimately lower the actuation energy needed below the energy needs of conventional ailerons. The mechanisms used it the first design was just one of many presented in Section 2.3. Other warping mechanisms and methods should be examined especially those which use smart materials that can be folded or rolled looking forward to integration with inflatable wings.

These designs should also be experimentally compared to conventional ailerons for drag and adverse yaw effects. The elimination of hinge lines and actuator systems exposed to the flow should have benefits for drag and adverse yaw.

The results in Chapter 6 show that the current wing design is capable of being integrated with a COTS autopilot system. Assuming future iterations of the design show similar flight characteristics and ease of integration with the autopilot, the project should begin looking at how the design can be integrated with inflatable wings. Hopefully due to the methods developed in this thesis the design of the mechanism will be matured to a point that the integration with the inflatable and with the autopilot is well understood and can become operational with minimal design-cycles.

BIBLIOGRAPHY

[1] Aerospace America , "2011 Worldwide UAV Roundup," [Online]. Available: http://www.aerospaceamerica.org/Documents/March%202011%20AA%20PDFs/UAV_CHART_2011.pdf. [Accessed 15 August 2012].

[2] K. Platoni, "Smithsonian Air & Space," [Online]. Available: http://www.airspacemag.com/flight-today/Thats-Professor-Global-Hawk.html. [Accessed 15 August 2012].

[3] NASA Dryden Flight Research Center, "Mission Update," [Online]. Available: http://www.nasa.gov/centers/dryden/news/Features/2007/wildfire_socal_10_07.html. [Accessed 15 August 2012].

[4] DIY Drones, [Online]. Available: www.DIYdrones.com. [Accessed 15 August 2012].

[5] Paparazzi , "Paparazzi The Free Autopilot," [Online]. Available: http://paparazzi.enac.fr/wiki/Main_Page. [Accessed 15 August 2012].

[6] Department of Defense, "Unmanned Aircraft Systems Roadmap," Washington DC, 2005.

[7] A. Bolonkin, "Estimated Benefits of Varibable-Geometry Wing Camber Control for Transport Aircraft," NASA, Edwards, 1999.

[8] C. O. Johnston, D. A. Neal, L. D. Wiggins, H. H. Robertshaw, W. H. Mason and D. J. Inman, "A Model to Compare the Flight Control Energy Requirements of Morphing and Conventionally Actuated Wings," Norfolk, 2003.

[9] H. M. Garcia, "Control of Micro Air Vehicles Using Active Wing Morphing," University of Florida, Gainsville, 2003.

[10] U.S. Centennial of Flight Commision, [Online]. Available:

10] http://www.centennialofflight.gov/sights/collections2.htm. [Accessed 18 August 2012].

F. E. C. Culick and H. R. Jex, "Aerodynamics, Stability and Control of the 1903 Wright
11] Flyer," AIAA, Los Angles, 1984.

O. Wright and W. Wright, "Flying-Machine". US Patent 821,393, 22 5 1906.
12]

G. D. Padfield and B. Lawrence , The birth of flight control: An engineering analysis of
13] the Wright brothers' 1902 glider, The Aeronautical Journal, 2003.

J. D. Jacob, "On the Fluid Dynamics of Adapative Airfoild," Anaheim, 1998.
14]

R. W. Guiler, "Control of a Swept Wing Tailless Aircraft through Wing Morphing,"
15] West Virginia University, Morgantown , 2007.

NASA, "AAW Fact Sheet," [Online]. Available:
16] http://www.nasa.gov/centers/dryden/news/FactSheets/FS-061-DFRC.html. [Accessed 20
August 2012].

S. Barbarino, O. Bilgen, R. M. Ajaj, M. I. Friswell and D. J. Inman, "A Review of
17] Morphing Aircraft," vol. 22, 2011.

A. D. Simpson, "Design and Performance of UAVs with Inflatable Wings," University of
18] Kentucky, Lexington, 2008.

W. K. Loh, "Deployment Dynamics of Inflatable Wings," Oklahoma State University,
19] Stillwater, 2006.

M. Abdurahim, H. Garcia, G. F. Ivey and R. Lind, "Flight Testing A Micro Air Vehicle
20] Using Morphing For Aeroservoelastic Control," AIAA, Gainsville, 2004.

H. Garcia , M. Abdulrahim and R. Lind, "Roll Control for a Micro Air Vehicle Using
21] Active Wing Morphing," AIAA - Guidance, Navigation and Control Conference, Austin, 2003.

D. A. Neal III, "Design, Development, and Analysis of a Morphing Aircraft Model for
22] Wind Tunnel Experimentation," Virginia Polytechnic Institue and State University,
Blacksburg, 2006.

D. A. Neal, M. G. Good, C. O. Johnston, H. H. Robertshaw, W. H. Mason and D. J.
23] Inman, "Design and Wind-Tunnel Analysis of a Fully Adaptive Aircraft Configuration," Palm
Springs, 2004.

M. Majji, O. K. Rediniotis and J. L. Junkins, "Design of a Morphing Wing: Modeling and
24] Experiments," College Station, 2006.

D. Cadogan, T. Smith, F. Uhelsky and M. MacKusick, "Morphing Inflatable Wing
25] Development for Compact Package Unmanned Aerial Vehicles," AIAA, 2004.

D. Cadogan, W. Graham and T. Smith, "Inflatable and Rigidizable Wings for
26] Unmanned Aerial Vehicles," Norfolk, 2003.

O. Bilgen, "Macro Fiber Composite Actuated Unmannned Air Vehicles: Design,
27] Development, and Testing," Virginia Tech, Blacksburg, 2007.

T. Sicdaniel, "Flying-Machine". US Patent 1905298, 13 August 1930.
28]

B. W. Cocke, "Wind tunnel investigation of the aerodynamic and strucural deflection
29] characteristics of the Goodyear Infltatoplane," NASA Langley Aeronautical Laboratory,
Langley Field, 1958.

T. Harris, "Constrained Volume Pakcing of Deployable Wing for Unmanned Aircraft,"
30] UK, Lexington, 2011.

A. Simpson, J. Jacob and S. Smith, "Inflatable and Warpable Wings for Meso-scale
31] UAVs," Washington DC, 2005.

M. J. Scott, J. D. Jacob, S. W. Smith and L. T. Asheghian, "SUAVE: A Low Stored Volume
32] High-Altitude Wing," NextGen Aeronautics, Torrance , 2009.

L. Asheghian, J. N. Kudva, J. Jacob, S. Smith and R. Kapania, "Stowed Unmanned Air
33] Vehicle Eningeering (SUAVE) Phase II," NextGen Aeronautics , Torrance, 2008.

W. P. Phillips, Mechnics of Flight 2nd edition, Hoboken: John WIley & Sons, 2010.
34]

J. Becker, "Piccolo Doublet Analysis Tool," Cloud Cap Technologies , Hood River, 2000.
35]

W. Durham, "Chapter 6 Forces and Moments," Virginia Tech Department of
36] Aerospace   and   Ocean   Engineering,   [Online].   Available:
http://www.dept.aoe.vt.edu/~durham/AOE5214/. [Accessed 31 August 2012].

J. Elston, M. Stachura, C. Dixon and T. Gerritsen, "NexSTAR RC to UA Conversion
37] Guide," University of Colorado - Boulder, 2009.

A. L. Houston, B. Argrow, J. Elston and J. Lahowetz, "Unmanned Aircraft Observations
38] of Airmass Boundaries: The Collaborative Colorado-Nebraska Unamnned Aircraft System
Experiment," 2008.

A. G. Ritchie, "Recent Advances in Lithium Ion Battery Materials," vol. 136, no. 2,
39] 2004.

E. W. Frew and T. X. Brown, "Airborne Communication Networks for Small Unmanned
40] Aircraft Systems," 2008.

R. Jager, "Test and Evaluation of the Piccolo II Autopilot System on a One-Third Scale
41] Yak-54," Auburn University, Auburn, 2005.

Academy of Model Aeronautics AMA, 16 July 2011. [Online]. Available:
42] http://www.modelaircraft.org/files/560.pdf. [Accessed 19 July 2012].

Academy of Model Aeronautics AMA, "Academy of Model Aeronautics AMA," AMA, 1
43] January 2011. [Online]. Available: http://www.modelaircraft.org/files/105.PDF. [Accessed
19 June 2012].

M. A. Thamann, "Aerodynamics and Control of a Deployable Wing UAV for
44] Autonomous Flight," University of Kentucky, Lexington, 2012.

D. P. Raymer, Aircraft Design a Conceptual Approach 4th edition, AIAA , 2006.
45]

J. Wanber, Composite Materials: Fabrication Handbook #1, Wolfgang Publications,
46] Inc., 2009.

J. Lambie, Composite Construction for Homebuilt Aircraft, Markowski Intl, 1996.
47]

J. Manor, "Dynamic Soaring - Carbon Testing," [Online]. Available:
48] http://www.rcgroups.com/forums/showthread.php?t=778363. [Accessed 21 July 2012].

M. W. Kehoe, "Aircraft Flight Flutter Testing at the NASA Ames-Dryden Flight
49] Research Facility," NASA, Edwards, 1988.

G. Brown, R. Haggard and B. Norton, "Inflatable Structures for Deployable Wings,"
50] AIAA, Lake Elsinore, 2001.

J. D. Jacob, A. Simpson and S. Suzanne, "Design and Flight Testing of Inflatable Wings
51] with Wing Warping," Society Automotive Engineers SAE, 2005.

VITA

1. Place of birth: Morehead, Kentucky

2. Educational Institutions attended and degrees already awarded:
Bachelor of Science in Mechanical Engineering, May 2010,
University of Kentucky, Lexington, KY

3. Professional positions held:

4. Scholastic and professional honors: 2010 Astronaut Scholar at the University of Kentucky, award from Astronaut Scholarship Foundation

5. Professional Publications:

6. Student Name: Edward Brady Doepke